Journal of Photochemistry and Photobiology B: Biology xxx (2011) xxx–xxx

Contents lists available at ScienceDirect

Journal of Photochemistry and Photobiology B: Biology

journal homepage: www.elsevier.com/locate/jphotobiol

Photosystem II fluorescence lifetime imaging in avocado leaves: Contributions of the lutein-epoxide and violaxanthin cycles to fluorescence quenching

Shizue Matsubara [a,*], Yi-Chun Chen [b], Rosanna Caliandro [a], Govindjee [c,d,e], Robert M. Clegg [b,e,f]

[a] Institut für Pflanzenwissenschaften (IBG-2), Forschungszentrum Jülich, 52425 Jülich, Germany
[b] Department of Bioengineering, University of Illinois at Urbana-Champaign, 3120 Digital Computer Laboratory, MC-278, 1304 West Springfield Avenue, Urbana, IL 61801, USA
[c] Department of Biochemistry, University of Illinois at Urbana-Champaign, 419 Roger Adams Laboratory, 600 South Mathews Avenue, Urbana, IL 61801, USA
[d] Department of Plant Biology, University of Illinois at Urbana-Champaign, 265 Morrill Hall, 505 South Goodwin Avenue, Urbana, IL 61801, USA
[e] Center for Biophysics and Computational Biology, University of Illinois at Urbana-Champaign, 156 Davenport Hall, 607 South Mathews Avenue, Urbana, IL 61801-3080, USA
[f] Department of Physics, University of Illinois at Urbana-Champaign, 1110 W. Green Street, Urbana, IL 61801, USA

ARTICLE INFO

Article history:
Available online xxxx

Keywords:
Fluorescence lifetime imaging microscopy
Lutein
Lutein epoxide
Polar plot
Thermal energy dissipation
Xanthophyll cycle

ABSTRACT

Lifetime-resolved imaging measurements of chlorophyll *a* fluorescence were made on leaves of avocado plants to study whether rapidly reversible ΔpH-dependent (transthylakoid H^+ concentration gradient) thermal energy dissipation (qE) and slowly reversible ΔpH-independent fluorescence quenching (qI) are modulated by lutein-epoxide and violaxanthin cycles operating in parallel. Under normal conditions (without inhibitors), analysis of the chlorophyll *a* fluorescence lifetime data revealed two major lifetime pools (1.5 and 0.5 ns) for photosystem II during the ΔpH build-up under illumination. Formation of the 0.5-ns pool upon illumination was correlated with dark-retention of antheraxanthin and photo-converted lutein in leaves. Interconversion between the 1.5- and 0.5-ns lifetime pools took place during the slow part of the chlorophyll *a* fluorescence transient: first from 1.5 ns to 0.5 ns in the P-to-S phase, then back from 0.5 ns to 1.5 ns in the S-to-M phase. When linear electron transport and the resulting ΔpH build-up were inhibited by treatment with 3-(3,4-dichlorophenyl)-1,1-dimethylurea (DCMU), the major fluorescence intensity was due to a 2.2-ns lifetime pool with a minor faster contribution of approximately 0.7 ns. In the presence of DCMU, neither the intensity nor the lifetimes of fluorescence were affected by antheraxanthin and photo-converted lutein. Thus, we conclude that both antheraxanthin and photo-converted lutein are able to enhance ΔpH-dependent qE processes that are associated with the 0.5-ns lifetime pool. However, unlike zeaxanthin, retention of antheraxanthin and photo-converted lutein may not by itself stabilize quenching or cause qI.

1. Introduction

Adaptation of photosynthetic organisms to terrestrial environments necessitated, among other things, the ability to rapidly regulate harvesting of light energy in response to dramatic changes in irradiance. Photosystem (PS) II complex, the light-driven water-plastoquinone oxidoreductase [1], is especially vulnerable to over-excitation and photooxidative damage because of its relatively slower photochemical turnover, combined with a large pool of chlorophyll (Chl) molecules bound in the major light-harvesting antenna complex (LHCII). Light energy absorbed in excess of photochemical utilization can be dissipated quickly and harmlessly in light-harvesting antenna complexes; this dissipation is triggered by a build-up of a transthylakoid H^+ concentration gradient (ΔpH) and involves de-epoxidized xanthophylls in the xanthophyll cycle (for review, see [2,3]). In the xanthophyll cycle, also termed violaxanthin (V) cycle, V is de-epoxidized to antheraxanthin (A) and zeaxanthin (Z) by the enzyme V de-epoxidase, which is activated by light-driven acidification of the thylakoid lumen. The reverse reactions catalyzed by Z epoxidase convert Z and A back to V and this becomes detectable when V de-epoxidase is inactive at high lumen pH, which usually occurs under weak light or during the night. The light-dependent de-epoxidation and epoxidation thus

Abbreviations: A, antheraxanthin; α-car, α-carotene; β-car, β-carotene; CCD, charge coupled device; Chl, chlorophyll; Chl *a*/Chl *b*, chlorophyll *a* to chlorophyll *b* ratio; DCMU, 3-(3,4-dichlorophenyl)-1,1-dimethylurea; ΔpH, transthylakoid proton concentration gradient; DPS, extent of de-epoxidation state of xanthophyll-cycle pigments; FLIM, fluorescence lifetime imaging microscopy; L, lutein; Lx, lutein epoxide; *M*, fractional depth of fluorescence modulation; NPQ, non-photochemical fluorescence quenching; φ, phase shift of the fluorescence modulation relative to the excitation modulation; PS, photosystem; qE, rapidly reversible ΔpH-dependent fluorescence quenching; qI, slowly reversible fluorescence quenching associated with photoinhibition; qT, fluorescence quenching associated with state transition (change in distribution of antenna between the two photosystems); V, violaxanthin; Z, zeaxanthin.

* Corresponding author. Tel.: +49 2461 61 8690, fax: +49 2461 61 2492.
E-mail address: s.matsubara@fz-juelich.de (S. Matsubara).

1011-1344/$ - see front matter © 2011 Elsevier B.V. All rights reserved.
doi:10.1016/j.jphotobiol.2011.01.003

determine the equilibrium position of V, A and Z, or de-epoxidation state (DPS) of the V cycle (DPS-VAZ) defined as DPS-VAZ = ([A] + [Z])/([V] + [A] + [Z]), where [V], [A] and [Z] refer to measured mmol amounts of V, A and Z per mol of Chl *a*. Elimination of V de-epoxidase activity by an inhibitor [4] or by genetic mutation [5] largely diminishes ΔpH-induced thermal energy dissipation, highlighting an essential role of the V cycle in light harvesting regulation. Indeed, the V cycle has been found in chloroplasts of all higher-plant species thus far investigated.

Some higher-plant species possess another xanthophyll cycle, involving lutein (L) and lutein epoxide (Lx), in addition to the V cycle (for a review of the Lx cycle, see [6]). Lutein epoxide undergoes light-induced de-epoxidation from Lx to L in the same way as V to A and Z. However, epoxidation of L to Lx is generally much slower than the corresponding reactions in the V cycle, and the kinetics of post-illumination Lx recovery are strikingly variable in different Lx-cycle species [6]. Nevertheless, substantial amounts of Lx can accumulate in leaves of Lx-cycle plants under shade (low light). While little Lx is detected in leaves of many plants, L, the other pigment in the Lx cycle, is universal and also the most abundant xanthophyll in higher-plant thylakoids. Involvement of L in thermal energy dissipation has been suggested by studies on *Arabidopsis* mutants either lacking or over-accumulating L [7–9] as well as in isolated LHCII and LHCII crystals [10,11]. Given this proposed role of L in energy dissipation, and also considering the analogous light-dependent responses and similar chemical structures of the xanthophyll molecules in the two cycles, we suggest that the operation of the Lx cycle is an additional mechanism for regulating light harvesting in the antenna complexes of the Lx-cycle plants [6]. In support of this notion, leaves maintaining high DPS in the Lx cycle (DPS-LxL, calculated as DPS-LxL = [L]/([Lx] + [L]), where [L] and [Lx] are mmol of L and Lx per mol of Chl *a*) after light-induced de-epoxidation, showed rapid and enhanced non-photochemical quenching (NPQ) upon re-illumination [12,13].

There are two opposing views concerning consequences of slow Lx restoration and the resulting retention of high DPS-LxL in leaves. One view is that high DPS-LxL leads to constitutive dissipation (down-regulation) in PSII both in the light and in the dark [14,15]. This resembles the reduced maximal PSII efficiency measured in overwintering leaves that accumulate large amounts of Z due to sustained de-epoxidation in the V cycle [16,17], or in leaves and cells of mutants that lack Z epoxidase activity [5,18–21]. The other view postulates that high DPS-LxL enhances energy dissipation under illumination, without affecting the maximal PSII efficiency in the dark [12]. In both cases, retention of high DPS-LxL is associated with rapid development of thermal energy dissipation upon irradiance increase.

The Chl *a* fluorescence intensity and lifetime signals change significantly during light induction, which is known as the Chl *a* fluorescence transient (for review of fluorescence induction, see [22,23]). These changes in fluorescence intensity reflect changes in PSII photochemistry, downstream reactions in the electron transport chain and CO_2 fixation, as well as protective or photoinhibitory thermal energy dissipation. The fluorescence induction curve begins with a minimum fluorescence level designated as O ('origin'), that rises to P ('peak'), followed by a decline to S ('steady state') within about a second; this is followed by a slow rise to M ('maximum') and a decline to T ('terminal state'). The detailed pattern depends on the intensity of excitation light. The patterns of the fluorescence transient vary among different photosynthetic organisms and are affected by photochemical reactions (dominant within the microsecond to second time window, represented by the O-to-P phase) as well as by physiological processes (within the second-to-minute time window, represented by the P–S–M–T phase) under given conditions. The Chl *a* fluorescence transient in different photosynthetic systems has been reviewed [23].

Most previous studies have analyzed the effect of the V and Lx cycles on light energy utilization and energy dissipation by measuring the Chl *a* fluorescence intensities. However, intensity measurements alone cannot distinguish between changes in Chl *a* concentrations or changes in fluorescence quantum yields (fluorescence lifetimes) caused by dynamic quenching reactions. To gain maximum information concerning underlying molecular mechanisms and concentration changes from fluorescence measurements, it is essential to measure fluorescence lifetimes [24]. Fluorescence lifetime-resolved measurements can differentiate Chl *a* species with different dynamic de-excitation rates (lifetimes), and importantly, *fluorescence lifetimes are independent of the concentrations of fluorophores*. Therefore, by determining lifetimes, it is possible to estimate fractional species concentrations from fractional intensity contributions of the different lifetime components (e.g. quenched and unquenched). Whether sustained de-epoxidation in the Lx cycle increases the rate constant of thermal energy dissipation in darkness (without ΔpH) and/or in light (with ΔpH) can be tested by measuring PSII Chl *a* fluorescence lifetimes at various DPS-LxL with different levels of ΔpH. Because changes in measured fluorescence parameters take place rapidly in photosynthetic systems during and following illumination, it is necessary to carry out the lifetime-resolved measurements rapidly [25]. In addition, we are interested in intact, fully functional photosynthetic systems. Therefore, we have used a real-time, full-field, frequency-domain, fluorescence lifetime-resolved imaging microscope (FLIM) to track real-time changes in the nanosecond fluorescence response in intact leaves of avocado plants. Avocado plants is an Lx-cycle species which shows extremely slow epoxidation. The goal of our experiments was to study changes, in real time, of relative concentrations of quenched and unquenched Chl *a* molecules in leaves of avocado plants with intact functional photosynthetic systems during illumination and following dark adaptation. Changes in concentrations of quenched and unquenched Chl *a* molecules during the fluorescence transient were quantified by following the dynamic fluorescence decay of Chl *a*.

Our lifetime-resolved fluorescence data reveal two major pools of PSII fluorescence lifetimes in avocado leaves: 1.5 ns and 0.5 ns (unquenched and quenched components). Dynamic interconversion between these two pools takes place during the Chl *a* fluorescence transient. Retention of L in the Lx cycle and A in the V cycle enhances rapid development of ΔpH-dependent quenching (termed qE) associated with the 0.5-ns lifetime pool; however, unlike Z, retention of A and L may not stabilize quenching in the absence of ΔpH. With DCMU, which blocks electron flow from reduced Q_A to the plastoquinone pool, the major lifetime pool was located at 2.2 ns with a minor intensity component at approximately 0.7 ns in all samples having various DPS in the two cycles. Our results lead us to conclude that both photo-converted L as well as A are involved in the ΔpH-dependent interconversion between the 1.5-ns and 0.5-ns lifetime pools in avocado leaves. To our knowledge, this is the first time FLIM measurements have been used to follow in real time lifetime changes due to both qE and qI.

2. Material and methods

2.1. Plant material

Two avocado trees (*Persea americana* Mill., var. 'Stuart Mexicola') were kept under room light (photosynthetic photon flux density of ~5 μmol photons m^{-2} s^{-1}) in the laboratory after they had been transported from a nursery (Clifton's nursery, Porterville, CA, USA) to the Physics Department of the University of Illinois at Urbana-Champaign. Following three weeks of 'acclimation', experiments were conducted by using fully-expanded, mature leaves.

Please cite this article in press as: S. Matsubara et al., Photosystem II fluorescence lifetime imaging in avocado leaves: Contributions of the lutein-epoxide and violaxanthin cycles to fluorescence quenching, J. Photochem. Photobiol. B: Biol. (2011), doi:10.1016/j.jphotobiol.2011.01.003

2.2. Light treatment

Since many genes in photosynthesis are controlled by circadian clocks (see e.g. [26]), we started measurements early in the morning. Leaves that had been kept in dim light of the laboratory were taken at 8:30 AM, cut into two halves along the midvein and floated on water with the adaxial surface facing the air. For each leaf, one half was placed under a halogen lamp (400–500 μmol photons m^{-2} s^{-1}, "*light*"-samples) for 20 min to induce xanthophyll de-epoxidation, while the other half was kept under room light (~5 μmol photons m^{-2} s^{-1}, "*control*"-samples). At the end of the treatment, both *light*- and *control*-samples were wrapped in a moist tissue and put in a plastic bag to avoid dehydration. Subsequently, they were kept in darkness to allow epoxidation of de-epoxidized xanthophylls.

Leaf discs (50 mm^2) for FLIM measurements were taken from *light*- and *control*-samples at five different time points (Fig. 1). After leaves had been collected at 8:30 AM, the first leaf discs of *control*-samples were taken and dark-adapted on a moist tissue for 10 min. These discs, called "*control*-morning", are in the most epoxidized state of the two xanthophyll cycles in avocado leaves in our experiment. After the 20-min treatment under the room light or the halogen lamp, leaf discs were taken in parallel from both *control*- and *light*-samples at four different time points during the subsequent dark recovery treatment in the plastic bag, namely after 10 ("*control*-10" and "*light*-10"), 60 ("*control*-60" and "*light*-60"), 180 ("*control*-180" and "*light*-180") or 360 ("*control*-360" and "*light*-360") min. The *light*-samples from the dark recovery treatment have different DPS of the V cycle.

2.3. Treatment with inhibitor

The ΔpH-dependence of the quenching was examined by treating the samples with 3-(3,4-dichlorophenyl)-1,1-dimethylurea (DCMU), which blocks electron flow from reduced Q_A (bound primary quinone in PSII) to the plastoquinone pool by displacing Q_B from its binding site [27], thereby inhibiting photochemical fluorescence quenching and the ΔpH build-up through linear electron transport. Two avocado leaves were collected at 8:30 AM and floated on water without being cut into two halves. One of the leaves was treated as *light*-sample while the other was treated as *control*, but both in the absence of DCMU, according to the treatment protocol described above. Following the different treatments, six replicate leaf discs (50 mm^2) were removed from both *light*- and *control*-leaves and three discs were floated on water (*water-control* and *water-light*) and the other three on 1.2 mM DCMU (*DCMU-control* and *DCMU-light*) with the adaxial surface facing the air for 360 min, corresponding to the longest dark recovery treatment of the time-course experiment. During the inhibitor treatment, the samples were kept under room light (~5 μmol photons m^{-2} s^{-1}). At the end of the inhibitor treatment, leaf discs were dark-adapted for 10 min and used for FLIM measurements.

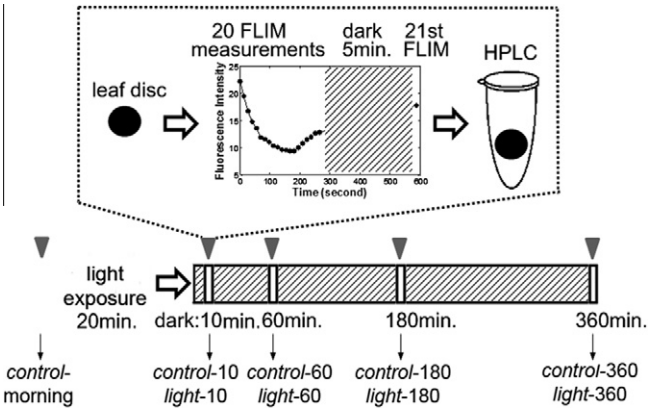

Fig. 1. Experimental protocol for FLIM (fluorescence lifetime imaging microscopy) measurements. Leaf disc samples of avocado plants were collected and FLIM measurements were performed at five different time points indicated by gray triangles. The first discs ("*control*-morning" samples) were taken after harvesting the leaves at 8:30 AM under room light (~5 μmol photons m^{-2} s^{-1}) and after dark adaptation for 10 min. All other samples were taken after a 20-min exposure of the leaves to room light (*control*-treatment) or halogen lamp (400–500 μmol photons m^{-2} s^{-1}, *light*-treatment) followed by dark adaptation of 10 ("*control*-10" and "*light*-10"), 60 ("*control*-60" and "*light*-60"), 180 ("*control*-180" and "*light*-180") or 360 ("*control*-360" and "*light*-360") min. Twenty consecutive FLIM measurements were made on each dark-adapted leaf disc under continuous laser illumination (50 μmol photons m^{-2} s^{-1}). After the 20th measurement, the laser beam was blocked for 5 min to dark-adapt the sample, and then the final (21st) measurement was made in the same spot. Then, leaf discs were dark-adapted for another 5 min and frozen in liquid nitrogen for pigment analysis by HPLC (High Performance Liquid Chromatography) (see Section 2.6).

2.4. Fluorescence lifetime imaging microscopy (FLIM) measurements

Full-field fluorescence lifetime-resolved images were obtained by the frequency-domain homodyne technique. The instrument is described elsewhere [19,28]. This method of measuring FLIM is rapid and all pixels on the CCD (Charge Coupling Device) are acquired simultaneously. The laser excitation wavelength was 488 nm for all FLIM measurements in this study, and the incident laser intensity on the sample surface was ~50 μmol photons m^{-2} s^{-1}. An emission filter with bandpass between 670 and 725 nm was used to collect mostly PSII fluorescence.

At room temperature, the contribution of PSI fluorescence is very little at all wavelengths [29]. In the frequency domain the lifetime components are weighted by their intensity contributions, and the intensity of a fluorescence species decreases proportionally as the lifetime decreases. The fluorescence of PSI decays in about 100 ps at room temperature; thus we do not expect to observe any dynamic fluorescence contribution from the PSI rapid decay. In accordance with this expectation, the progression of the points on the polar plot (Section 2.5) during the FLIM data acquisition (Section 3.3, shown later in Fig. 6) shows no deviation toward the fast lifetime of PSI as the 0.5-ns lifetime pool is approached. Spectrally resolved FLIM measurements between 690 and 700 nm focused on PSII [28] show similar results as reported here. Thus, the PSI component is negligible in our measurements.

Dark-adapted leaf discs were placed between a cover slip and moist tissue, which was put on a glass slide. Fluorescence intensity images were obtained with a 40× objective lens from the adaxial surface of the leaf discs, focusing on a mesophyll layer. Fig. 2A shows a fluorescence intensity image of an avocado leaf disc. The gray scale bar represents fluorescence intensity (in arbitrary units, A.U.). The structure of veins (dark areas) and chloroplasts (bright spots) can be distinguished easily in this image.

The measurement protocol adopted for the FLIM experiments in this study is shown in Fig. 1. Twenty consecutive FLIM measurements were made under continuous laser illumination (488 nm) to determine phase (φ) and modulation (M) values (which are related to the lifetimes – see Section 2.5) and intensity during the fluorescence induction transient. Each measurement took 15 s. After 300 s (that is, following the 20th FLIM measurement), the laser light was blocked for 5 min to dark-adapt the sample, followed by a final (21st) FLIM measurement at the same spot. The purpose of this last measurement was to check if the laser illumination caused slowly reversible quenching associated with photoinhibition (qI).

After the 21st measurement, leaf discs were dark-adapted for another 5 min to minimize a local effect of laser illumination before being frozen in liquid nitrogen (77 K) for later High Performance Liquid Chromatography (HPLC) pigment analysis.

Please cite this article in press as: S. Matsubara et al., Photosystem II fluorescence lifetime imaging in avocado leaves: Contributions of the lutein-epoxide and violaxanthin cycles to fluorescence quenching, J. Photochem. Photobiol. B: Biol. (2011), doi:10.1016/j.jphotobiol.2011.01.003

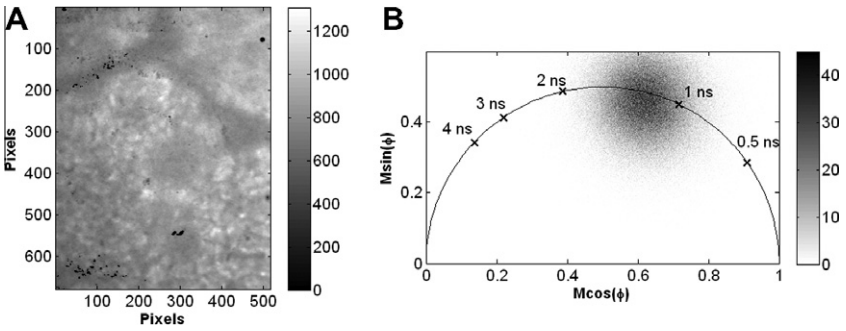

Fig. 2. FLIM measurement of an intact avocado leaf disc. (A) Chl *a* fluorescence intensity image of a 1st FLIM measurement on a *light-360* sample. A 40× objective lens is used and focused on a mesophyll cell layer. The gray scale bar represents fluorescence intensity (in arbitrary units). (B) Polar plot ($M\cos(\varphi)$ versus $M\sin(\varphi)$, where M and φ are modulation and phase) representation of the fluorescence lifetime information of every pixel of the image in panel A. The gray scale bar indicates the number of pixels.

2.5. Frequency domain data analysis and the polar plot analysis

Data from FLIM measurements were analyzed by using a digital Fourier transform algorithm [30] to determine the measured frequency-domain fluorescence lifetime parameters, M and φ, at every pixel. M is the amplitude of the AC modulation of the fluorescence signal relative to the DC average of the fluorescence; φ is the phase delay of the fluorescence relative to the excitation light. For a single lifetime component, these parameters are related directly to the lifetime as follows:

$$M = \frac{1}{\sqrt{1+(\omega\tau)^2}}, \quad (1)$$

$$\varphi = \tan^{-1}(\omega\tau), \quad (2)$$

where ω is modulation frequency of the instrument, which was 100 MHz in this study, and τ is the fluorescence lifetime of the fluorophore. For the case of multiple lifetime components, the fluorescence signal is still modulated at the same frequency as the excitation light, but lifetimes determined from the measured modulation and phase values in Eqs. (1) and (2) are only effective lifetimes, and do not refer to actual individual lifetimes. However, information concerning the individual contributing lifetimes can still be determined by well-known methods [30].

The fluorescence lifetime data were analyzed by the model-free, "*polar plot*" method [28,31,32] to identify differently quenched states of Chl *a* molecules, and the behavior of the different quenched states was followed during the light induction. Model-free means that no models are assumed and no analysis is carried out prior to the construction of the polar plot (for instance, no assumption of the number of fluorescence components is made). The modulation and phase parameters, which are measured in a model-free manner in the frequency domain data acquisition, are directly plotted. Thus the fluorescence response during the fluorescence transient is tracked directly on the polar plot without the previous intervention of a model. In this plot, the *x*- and *y*-axes are defined as

$$x = M\cos(\varphi), \quad (3)$$

$$y = M\sin(\varphi). \quad (4)$$

Fig. 2B shows the polar plot analysis of all the pixels from Fig. 2A. For *in vivo* experiments on intact leaves, fluorescence lifetime parameters were calculated by averaging lifetime data from a center area of a full-field image. The CCD exposure time was selected to achieve a good signal-to-noise ratio.

The advantage of the polar plot representation is that it displays the two fluorescence lifetime-related parameters, M and φ, on the same figure, with $M\cos(\varphi)$ and $M\sin(\varphi)$ on the *x*- and *y*-axis, respectively. The semicircle is centered at $(x, y) = (0.5, 0)$ and has a radius of 0.5. The polar plot provides a direct visualization and characterization of lifetime data without *a priori* assuming a model [28,31]; that is, without an initial assumption of the number or distribution of fluorescence lifetime components. All (x, y) points representing a fluorescence signal from a fluorophore with a single lifetime lie on a universal semicircle of the polar plot. All points from a fluorescence signal composed of multiple lifetime components lie inside the semicircle. Data points from fluorescence with two lifetime components are inside the semicircle and lie on a straight line connecting the two single lifetime locations on the semicircle. The position on the straight line depends on the fractional fluorescence intensity contributed by each lifetime component [31].

2.6. Pigment analysis

These data, determined from fluorescence lifetime-resolved measurements, were compared with the levels of DPS-LxL and DPS-VAZ for each sample, determined by HPLC, to correlate the quenching effect of xanthophyll de-epoxidation with the molecular composition of the two cycles. Leaf discs (50 mm^2), frozen in liquid nitrogen following the FLIM experiments, were lyophilized overnight. Immediately before pigment extraction, leaf discs were ground in a small amount of liquid nitrogen by using a mortar and pestle. Pigments were extracted in chilled acetone, and the final volume of the extract was adjusted to 1 mL. Then the extracts were centrifuged at 13,000 rpm for 5 min and syringe-filtered prior to the HPLC analysis.

Photosynthetic pigments were separated on an Allsphere ODS-1 column (5 μm, Alltech Associates, Deerfield, IL, USA) using solvents and protocols modified from Gilmore and Yamamoto [33]. Pigments were identified by retention times and absorption spectra monitored by a Waters 996 photodiode array detector (Waters Corporation, Milford, MA, USA). Data were analyzed with Waters Empower software. The HPLC system was calibrated for quantitative analysis of carotenoids and Chls by using pure standards (Chls from Sigma Aldrich Chemie, Taufkirchen, Germany; carotenoids from CaroteNature, Lupsingen, Switzerland).

3. Results

3.1. Pigment composition in avocado leaves before and after various light treatments

The photosynthetic pigment composition of dark-adapted avocado leaves taken at 8:30 AM ("*control*-morning" samples) is

Please cite this article in press as: S. Matsubara et al., Photosystem II fluorescence lifetime imaging in avocado leaves: Contributions of the lutein-epoxide and violaxanthin cycles to fluorescence quenching, J. Photochem. Photobiol. B: Biol. (2011), doi:10.1016/j.jphotobiol.2011.01.003

summarized in Table 1. The avocado leaves used here had a relatively high Chl *a* to Chl *b* ratio (Chl *a*/Chl *b* higher than 4), suggesting a somewhat small PSII antenna size. Neither Z nor A was detected in these dark-adapted samples; the V-cycle pigments were fully epoxidized to V. In contrast, only 10% of the Lx-cycle pigments were Lx and the rest were L. The majority of these L molecules were probably not involved in xanthophyll cycling, analogous to large pools of L found in plants without a Lx cycle, or to non-convertible pools of V in the V cycle [34]. As previously reported [15], avocado leaves contained substantial amounts of α-carotene (α-car), a pigment often found in shade-grown leaves or shade-tolerant plants (e.g. [35]). The total amount of carotenes (α-car + β-car), most of which are bound in the core complexes [36], was ca. 110 mmol per mol Chl; this is more than 50% of the total xanthophylls (about 200 mmol per mol Chl), which includes neoxanthin (N) in addition to V, Lx and L.

The 20-min exposure to the halogen lamp followed by 10-min dark adaptation (''*light*-10'') resulted in de-epoxidation of nearly half of the V-cycle pigments (Figs. 3A and B). The V level was gradually restored in the *light*-samples at the expense of A + Z during the subsequent dark period of 60, 180 and 360 min (*light*-60, *light*-180 and *light*-360, respectively); further, the recovery was not complete even after 6 h of darkness. Following different durations of dark adaptation, A was the dominant de-epoxidized form of V in *light*-samples.

The 20-min *light* treatment also induced de-epoxidation in the Lx cycle (Figs. 3C and D). The Lx level was diminished to less than 5 mmol per mol Chl in the *light*-10-samples, which was accompanied by an increase in DPS-LxL. Although a decrease in L has been documented in avocado leaves after transfer to much higher light intensities [15], the moderate intensity of the halogen lamp used for the light treatment did not cause such a decrease in L in our avocado leaves. Unlike the V cycle, the Lx cycle exhibited little recovery during subsequent dark adaptation of up to 6 h, in agreement with the slow reversibility of this cycle observed in avocado leaves in previous physiological/ecophysiological studies [6,15].

No change in pigment composition was detected in separate *control*-samples, which were kept under room light during the 20-min treatment (Fig. 3); that is, for these *control*-samples, the xanthophylls in both cycles remained epoxidized throughout the experiment.

3.2. Fluorescence lifetime imaging microscopy (FLIM) measurements in control- and light-samples

In the *control*- and *light*-samples showing different degrees of de-epoxidation due to contrasting epoxidation kinetics in the two cycles, FLIM measurements were made *in vivo* to examine the effects of xanthophyll de-epoxidation on the PSII Chl *a* fluorescence lifetime. Fig. 4 shows the average fluorescence intensity measured in three different leaves of *control*- (open symbols) and *light*-samples (closed symbols) during 20 consecutive FLIM measurements under continuous laser illumination. Note that the data of the 1st FLIM measurements, shown at time $t = 0$, were actually

Table 1
Pigment composition in dark-adapted avocado leaves in the morning.

Chl *a*/Chl *b*	N	V	Lx	L	α-car	β-car
4.16 ± 0.14	35.0 ± 1.6	32.4 ± 0.8	13.9 ± 2.4	117.3 ± 8.6	31.2 ± 3.1	80.9 ± 4.1

Carotenoid contents are given on a Chl basis (mmol mol Chl^{-1}). Neither A nor Z was detected in the samples. ($n = 4$, ±SE).

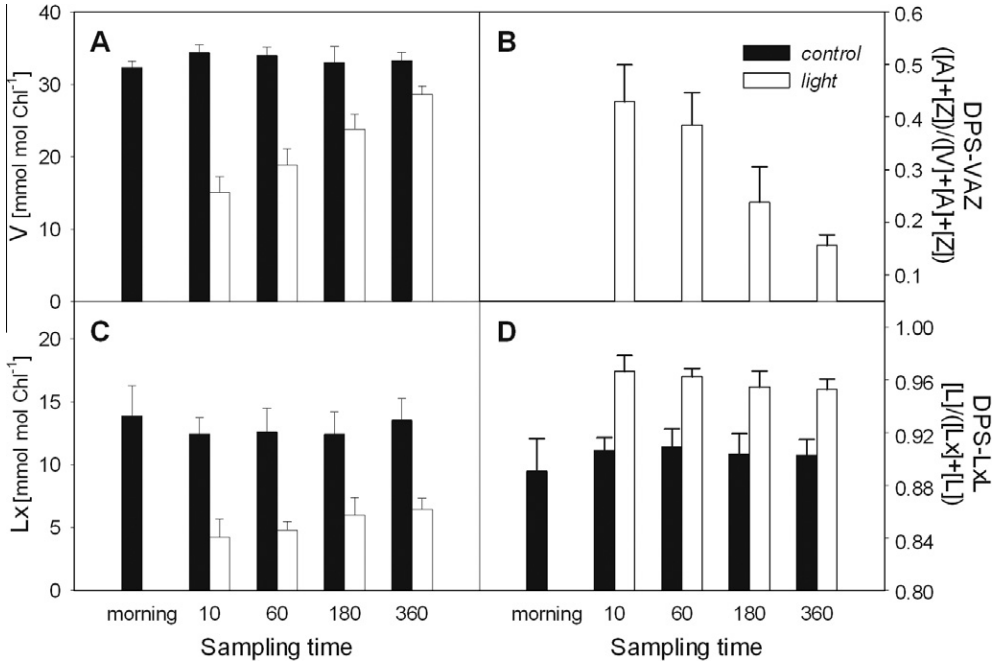

Fig. 3. Composition of the xanthophyll-cycle pigments in dark-adapted *control*- and *light*-samples at different times ($n = 4$, ±SE). (A) Levels of violaxanthin (V). (B) De-epoxidation state of the V cycle (DPS-VAZ) calculated as ([A] + [Z])/([V] + [A] + [Z]), where [V], [A] and [Z] are amounts of violaxanthin, antheraxanthin and zeaxanthin (mmol mol^{-1} Chl), respectively. (C) Levels of lutein epoxide (Lx). (D) De-epoxidation state of the Lx cycle (DPS-LxL) calculated as [L]/([Lx] + [L]), where L is lutein. The different sampling times were: at 8:30 AM and after 10, 60, 180 or 360 min of dark adaptation following a 20-min exposure to ~5 (*control*) or 400–500 μmol photons m^{-2} s^{-1} (*light*). None of the *control*-samples contained A or Z whereas most of the *light*-samples had A, but no Z, except for a single *light*-10-sample in which a small amount of Z (5.5 mmol mol^{-1} Chl) was detected.

Please cite this article in press as: S. Matsubara et al., Photosystem II fluorescence lifetime imaging in avocado leaves: Contributions of the lutein-epoxide and violaxanthin cycles to fluorescence quenching, J. Photochem. Photobiol. B: Biol. (2011), doi:10.1016/j.jphotobiol.2011.01.003

recorded during the first 15 s of illumination, and accordingly do not represent the maximum fluorescence intensity (Fm, measured in a dark-adapted state). The final (21st) measurement was made in the time interval between 600 and 615 s, following the 20 consecutive FLIM measurements and a 5-min dark adaptation.

In general, and as expected, the fluorescence intensity of the 1st measurements was higher in *control*-samples than in *light*-samples; the highest intensity was found in *control*-morning and the lowest in *light*-10 (Fig. 4). The initial fluorescence intensity upon illumination varied little among *control*-samples, whereas the intensity values increased in *light*-samples with increasing length of dark adaptation from 10 to 360 min. Pronounced recovery of the initial fluorescence intensity was observed in *light*-samples between 10 and 60 min of dark treatment; thereafter, the recovery was small.

After the 1st FLIM measurements, the fluorescence intensity initially decreased (corresponding to the P to S decline in the Chl *a* fluorescence transient) and then increased (corresponding to the S to M rise) in all samples under the continuous laser illumination. Independent of the light intensity during the pre-treatments, longer dark adaptation resulted in a slower onset of the S-to-M rise, which happened earliest in *light*-10 (after the 4th measurement) and latest in *control*-360 (the 19th measurement). In all samples except *light*-10, the fluorescence intensity of the 21st measurement recovered to 80% or 90% of the original values recorded at the 1st FLIM measurements, indicating that the 5-min laser illumination caused little qI in our avocado leaf discs. In the case of *light*-10 samples, the intensity of the 21st measurements was higher than the 1st measurements.

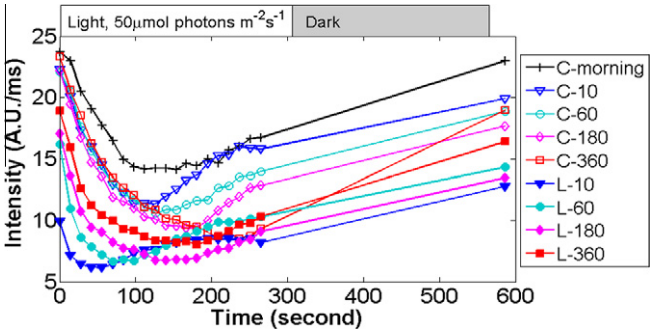

Fig. 4. Chlorophyll *a* fluorescence intensity during 20 continuous FLIM measurements under laser illumination (50 μmol photons m^{-2} s^{-1}) and a subsequent 21st measurement after 5 min of dark adaptation. Fluorescence intensity (in arbitrary units, A.U.) was normalized to a 1 ms CCD (Charge Coupled Device) exposure time. Shown are the averages of three replicates from three different leaves for *control*- (C, open symbols) and *light*-samples (L, filled symbols) at five different sampling times: morning, and after 10, 60, 180 or 360 min of dark adaptation following a 20-min exposure to ~5 (*control*) or 400 to 500 μmol photons m^{-2} s^{-1} (*light*).

3.3. Analysis of FLIM data

The FLIM data of *control*- and *light*-samples taken from one of three replicate leaves are presented in Fig. 5. Several locations corresponding to single lifetimes (4 ns, 3 ns, 2 ns, 1.75 ns, 1.19 ns, 0.70 ns and 0.46 ns) are marked for reference on the semicircle of the polar plot of Fig. 5. Comparable results were obtained in all replicate leaves. The data from *control*- and *light*-samples are located inside the semicircle, indicating that the fluorescence signals of these samples were composed of multiple lifetime components. The data of the complete sequence of FLIM measurements (during the fluorescence transients measured at different delay times) are fitted with a linear least-squares regression (Fig. 5). Each separate data sets of control and light samples fit well to a straight line, intercepting the semicircle at positions corresponding to a slower and faster lifetime. The intercept values on the polar plots varied slightly among the three controls and among the three light samples for the different leaves; but the overall behavior was the same. The averages and variances for the two semicircle intercepts from control and light sample data acquired with different leaves are: control: 1.70 (±0.10), 0.60 (±0.09); light: 1.28 (±0.09), 0.44 (±0.05). Both intercepts for the light samples correspond to somewhat faster lifetimes than the corresponding intercepts for the control samples. The reason for this is not known.

Fig. 6A shows the *control*- (blue open circles) and *light*-samples (red filled circles) of data and linear fit from all the different leaves on the same plot. By close inspection of this plot, it is clear that the control and light samples do not follow exactly the same straight line, as do the data from the separate leaves (e.g. Fig. 5). The straight line fit to the combined samples (all controls together with all light samples) intercepts the semicircle at locations corresponding to two lifetimes, at 1.56 ns and at 0.51 ns. However, these intercept values are very close to the average of the intercept values from Fig. 5.

For convenience in the following discussion of the data, we refer to the slower and faster lifetime components (pools) as the 1.5 and 0.5 ns components, for both the control and for the light samples, recognizing, of course, that these values are slightly different for the control and light samples of the different leaves. During the 5-min light induction, data from *control*-samples progress along this straight line, starting from positions near 1.5 ns and progressing towards 0.5 ns (Figs. 5A and 6A). Later during the light induction, the points on the polar plot gradually progress back along the straight line towards the 1.5-ns starting point. This pattern follows the P–S–M transient observed in the fluorescence intensity (Fig. 4); that is, shorter lifetimes correspond to lower fluorescence intensities, in agreement with a previous report in barley leaves [37]. This excellent correlation between the data acquired from fluorescence lifetime data and the measured fluorescence intensity strongly implies that the fluorescence transient arises from the interconversion of Chl *a* molecules between two major lifetime

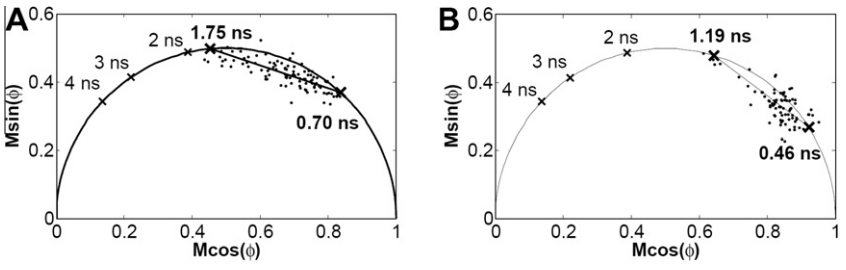

Fig. 5. Separate polar plots of FLIM data from (A) *control*- and (B) *light*-samples taken from one of the replicate leaves at five different time points: 8:30 AM, after 10, 60, 180 or 360 min of dark adaptation following a 20-min exposure to ~5 (*control*) or 400–500 μmol photons m^{-2} s^{-1} (*light*). As discussed in the text, the position on the regression straight line indicates the estimated intensity fractions of two lifetime pools with lifetimes of 1.75 ns and 0.70 ns for the control, and 1.19 ns and 0.46 ns for the light samples.

Please cite this article in press as: S. Matsubara et al., Photosystem II fluorescence lifetime imaging in avocado leaves: Contributions of the lutein-epoxide and violaxanthin cycles to fluorescence quenching, J. Photochem. Photobiol. B: Biol. (2011), doi:10.1016/j.jphotobiol.2011.01.003

pools (unquenched and quenched). Compared to *control*-samples, the polar plot data from *light*-samples are initially concentrated nearer to the 0.5-ns point on the semicircle (Figs. 5B and 6A), especially for the data of *light*-10. The same general pattern of data progression along the straight line was observed in the *light*-samples as in the *control*-samples. That is, during the 5-min light induction the data points first progressed along the straight line towards the 0.5-ns location, and then reversed, progressing towards the 1.5-ns location. This again parallels the intensity changes measured in these samples (Fig. 4). Fig. 6B shows a three-dimensional (3-D) polar plot of the same data set as in Fig. 6A, with the fluorescence intensity given on the *z*-axis. The 3-D representation shows that the rise and decay of the intensity along the *z*-axis (which is the same data as in Fig. 6C) correlates monotonically with the progression of the FLIM data along the straight line between the two lifetimes intersecting the semicircle on the *x*–*y* plane (the *x*–*y* plane is the polar plot of Fig. 6A).

In order to further examine the underlying mechanism of the observed fluorescence intensity changes, we used the measured lifetime parameters (lifetimes and fractional intensities) obtained from the polar plot analysis of the fluorescence intensity data (Fig. 6B) to simulate a two-lifetime model (see Appendix A, "*The two-lifetime model*" for a detailed derivation). In this model, we assume that the fluorescing molecules giving rise to the two different lifetime components have the same natural radiative lifetime; in other words, the two lifetimes represent two degrees of dynamic quenching of otherwise identical Chl *a* molecules. The two-lifetime model can distinguish between two different possibilities for the fluorescence intensity changes during the fluorescence induction: (1) shifts in fractional contributions of two lifetime components through interconversion between two quenched states (keeping the concentrations constant), or (2) changes in the total concentration of molecules capable of fluorescence. In Fig. 6C, the fluorescence intensity is plotted against the fractional intensity of the 0.5-ns lifetime pool, calculated by assuming a two-lifetime model (two pools centered around two different lifetimes) with variable fractional contributions. The data from both *control*- and *light*-samples are distributed along the simulation curve of the two-lifetime model, and the simulated fluorescence intensity agrees well with the measured intensity transient in these samples. The simulated values are close to the experimental data in all the individual samples at different time points (see Figure B.1 in Appendix B). These results demonstrate that the interconversion between the two differently quenched states, represented by the 1.5- and 0.5-ns lifetime pools in the polar plot, adequately explain the changes in fluorescence intensity observed in the avocado leaf discs during the P–S–M fluorescence transient (Fig. 4). Concentration changes of Chl, such as due to molecular degradation (photolysis) or state transitions (i.e. shuttling of light-harvesting antenna complexes between PSII and PSI) [38,39], appear to play a minor role in the quenching of fluorescence in avocado leaves under our experimental conditions.

Frequency domain FLIM measures directly "intensity fractions", which are the fractions of intensity that correspond to the different lifetimes. If the component lifetimes are known, the fractions of the molecular species with different lifetimes can be calculated. Fig. 7 summarizes the behavior of the "species fractions" of the two lifetime pools (1.5- and 0.5-ns pools) during the light induction in *control*- and *light*-samples. In all *control*-samples, laser illumination induced a very similar P-to-S fluorescence decrease in the fraction of Chl *a* species of the 1.5-ns lifetime pool (Fig. 7A); this decline was slightly slower in the *control*-morning samples. However, differences between the *control*-samples were observed in the subsequent S-to-M fluorescence rise. Longer dark treatment delayed the onset of the S-to-M fluorescence rise, concomitant with a progressive decrease of the lowest fraction of the 1.5-ns species measured during the light induction. In *control*-samples, the lowest species fraction of the 1.5-ns lifetime pool occurred between 180 and 195 s (*control*-morning, black crosses), 120 and 135 s (*control*-10, blue open triangles), 135 and 195 s (*control*-60, cyan open circles), 165 and 180 s (*control*-180, pink open diamonds), and 210 and 255 s (*control*-360, red open squares). At the 21st FLIM measurements after 5 min of darkness, the 1.5-ns species fraction recovered to 60–80% of the initial levels, analogous and corresponding to the intensity data (Fig. 4).

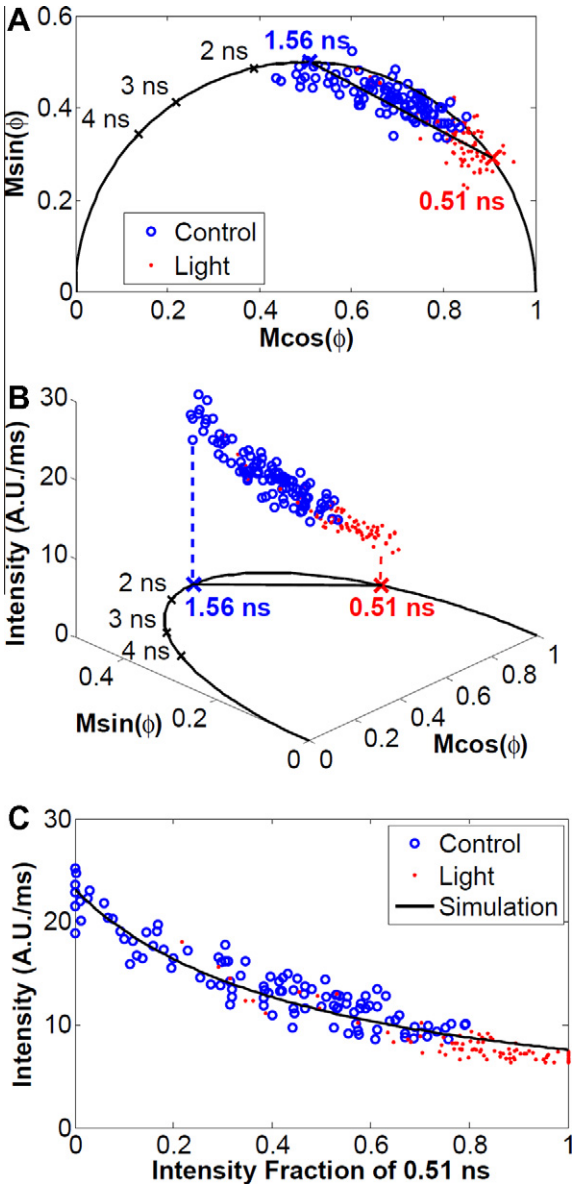

Fig. 6. Polar plot of FLIM combined data from both *control*- (blue open circles) and *light*-samples (red filled circles), (A) and (B); and fluorescence intensity against fractional intensity of a lifetime component (c). (A) The polar plot of all data from *control*- and *light*-samples taken from one of the three replicate leaves at five different time points: 8:30 AM, after 10, 60, 180 or 360 min of dark adaptation following a 20-min exposure to ~5 (*control*) or 400–500 μmol photons m^{-2} s^{-1} (*light*). The regression straight line indicates the estimated fractions of two lifetime pools with lifetimes of 1.5 ns and 0.5 ns. (B) A 3-D presentation of the polar plot; the *z*-axis is the fluorescence intensity normalized to CCD exposure time (arbitrary units, A.U. normalized to 1 ms). (C) Measured fluorescence intensity plotted against the fractional intensity of the 0.5-ns lifetime pool derived from the polar plot. The simulation (line) is calculated from the two-lifetime model (see text and Appendix A). (For interpretation of the references to colour in this figure legend, the reader is referred to the web version of this article.)

Please cite this article in press as: S. Matsubara et al., Photosystem II fluorescence lifetime imaging in avocado leaves: Contributions of the lutein-epoxide and violaxanthin cycles to fluorescence quenching, J. Photochem. Photobiol. B: Biol. (2011), doi:10.1016/j.jphotobiol.2011.01.003

The species fraction of the 1.5-ns lifetime pool was much smaller in *light*-samples than in *control*-samples, and this was observed already for the 1st FLIM measurements (Fig. 7B). The initial species fraction of the 1.5-ns pool recovered in *light*-samples with increasing duration of dark adaptation (from 10% to 50%). However, unlike in the *control*-samples, in all the *light*-samples the 1.5-ns species fraction decreased to comparable low levels (less than 10%) during the light induction, although this decrease was fastest in *light*-10 and slowest in *light*-360. These lowest values were recorded in *light*-samples between 30 and 45 s (*light*-10, blue filled triangles), 90 and 135 s (*light*-60, cyan filled circles), 120 and 195 s (*light*-180, pink filled diamonds), and 135 and 225 s (*light*-360, red filled squares). At the 21st measurements, the 1.5-ns species fraction accounted for about 40% of the entire population of the fluorescent molecules in all *light*-samples irrespective of the sampling time. Except in *light*-10, this corresponds to 80% of the initial levels.

The species fraction of the 0.5-ns lifetime pool undergoes changes essentially opposite to that of the 1.5-ns pool (Fig. 7C and D for *control*- and *light*-samples, respectively). This is also evident in Fig. A.2 in Appendix B, where the species fractions of the two lifetime pools are plotted together for each treatment and time.

3.4. Xanthophyll de-epoxidation state and the 0.5-ns lifetime pool

If the two xanthophyll cycles in avocado leaves are involved in regulation of light harvesting and thermal energy dissipation, variations in the species fraction of the two lifetime pools (Fig. 7) should correlate with changes in DPS (Fig. 3). In order to directly compare fluorescence lifetime and pigment data, the species fraction of the short (0.5-ns) lifetime pool was plotted against DPS for each sample (Fig. 8). As these DPS values represent a dark-adapted condition, only the lifetime data from the first three measurements (within 45 s) were examined, that is, only before substantial de-epoxidation could have been induced by laser illumination. The DPS was analyzed separately for the V cycle (DPS-VAZ, Fig. 8A–C) and the Lx cycle (DPS-LxL, Fig. 8D–F), as well as both cycles combined (DPS-all, calculated as ([A] + [L])/([V] + [A] + [Lx] + [L]), Fig. 8G–I). In these samples DPS-VAZ was determined by the levels of A and V; the data of the single *light*-10-sample, which contained some Z, was not included in Fig. 8.

Linear regression lines fitted to the data show a positive correlation between the species fraction of the 0.5-ns lifetime pool and DPS of each xanthophyll cycle separately, as well as both cycles together (Fig. 8). The 0.5-ns species fraction was best predicted by DPS-all, suggesting the involvement of both A in the V cycle and L in the Lx cycle in the interconversion between the 1.5- and 0.5-ns lifetime pools. The highest R^2 values were found at the 1st and 2nd measurements for DPS-all (Fig. 8B, E and H). In the first 15 s both DPS-VAZ and DPS-all explained the variations in the 0.5-ns species fraction well; thereafter, the correlation was better when the two cycles were combined than for the V cycle alone. Between the two cycles, DPS-VAZ indicated a stronger correlation with the 0.5-ns species fraction than DPS-LxL, which may be attributed to a greater impact of the V cycle than the Lx cycle, or the large pool of L that is not involved in the Lx cycle.

3.5. Inhibitor experiment

Unlike the qI-type quenching that persists in the absence of ΔpH, the rapidly reversible component of fluorescence quenching (qE) requires a build-up of ΔpH across the thylakoid membrane [40,41]. To ascertain the effect of ΔpH on fluorescence lifetimes, avocado leaf discs were treated with water or 1.2 mM DCMU during the 6-h recovery period following the 20-min *light*- or *control*-treatment in the absence of DCMU.

The FLIM measurements were performed in the water- or DCMU-treated leaf discs using the same measurement protocol. The fluorescence data of the water-treated leaf disc samples (brown circles in Fig. 9A) were very similar to those of *control*- and *light*-samples shown in Figs. 4–6. After incubation with DCMU, the fluorescence intensity and the lifetime parameters remained essentially constant in both *DCMU-light* and *DCMU-control* samples during laser illumination (green circles in Fig. 9). The minor variations in the lifetime data between the different samples were due to slight differences between the individual leaf discs, rather than light-induced changes in fluorescence lifetime in single leaf discs. The nearly complete absence of the P-to-S decay for each individual sample confirms the efficacy of the DCMU treatment. This is in

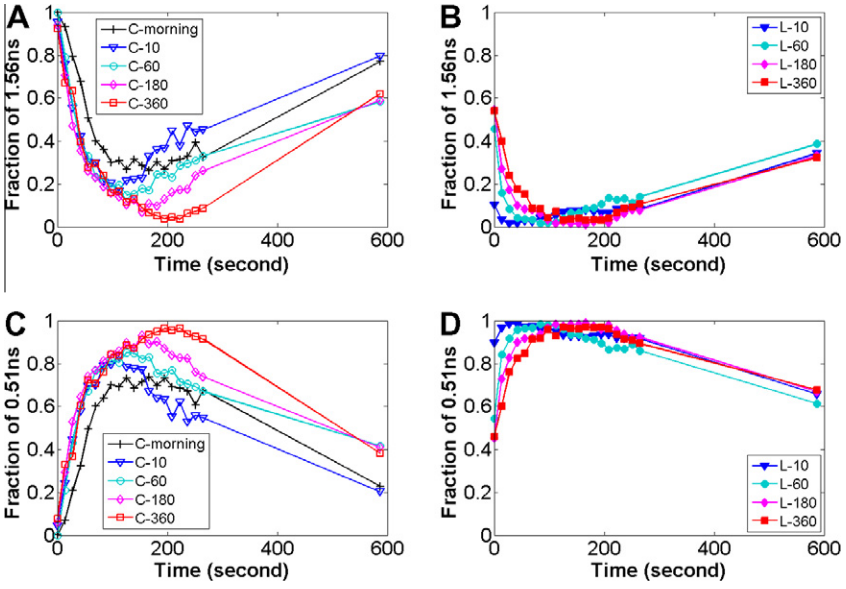

Fig. 7. Species fractions of the 1.5-ns (A and B) and 0.5-ns (C and D) lifetime pools during FLIM measurements; A and C are *control*-samples, and B and D are *light*-samples. Shown are the averages of three replicates from three different leaves for *control*- (C) and *light*-samples (L) at five different sampling times: 8:30 AM, after 10, 60, 180 or 360 min of dark adaptation following a 20-min exposure to ~5 (*control*) or 400–500 μmol photons m^{-2} s^{-1} (*light*).

Please cite this article in press as: S. Matsubara et al., Photosystem II fluorescence lifetime imaging in avocado leaves: Contributions of the lutein-epoxide and violaxanthin cycles to fluorescence quenching, J. Photochem. Photobiol. B: Biol. (2011), doi:10.1016/j.jphotobiol.2011.01.003

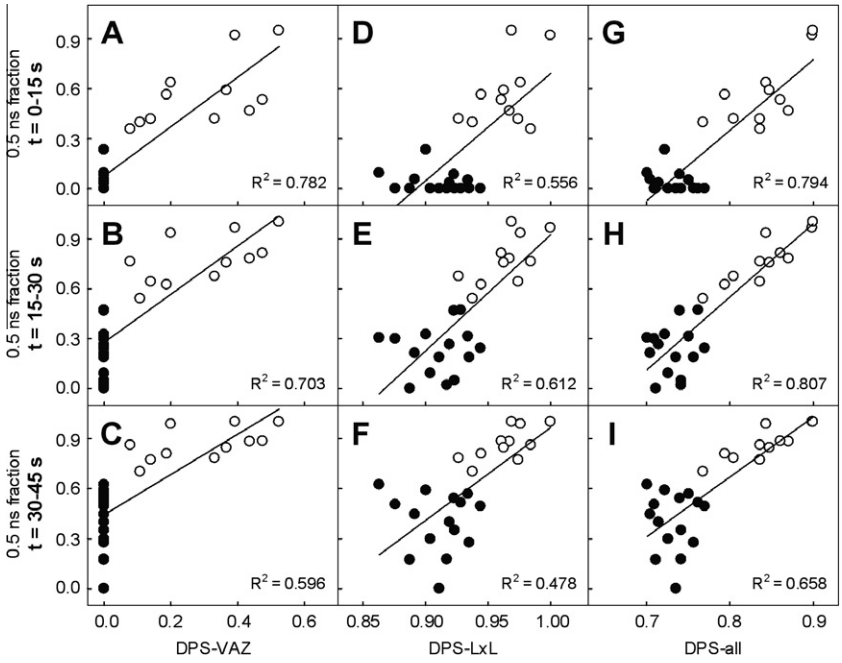

Fig. 8. Correlation between the de-epoxidation state (DPS) of the two xanthophyll cycles and the species fraction of the 0.5-ns lifetime pool in *control*- (black symbols) and *light*-samples (white symbols). (A–C) De-epoxidation state of the V cycle, DPS-VAZ; (D–F) de-epoxidation state of the Lx cycle, DPS-LxL; (G–I) combined de-epoxidation state of the two cycles, DPS-all. The species fractions at the 1st (0–15 s; A, D and G), 2nd (15–30 s; B, E and H) and 3rd (30–45 s; C, F and I) measurements of the 21 FLIM measurements are shown. Each symbol represents an individual leaf disc. DPS-VAZ is calculated as [A]/([V] + [A]) and DPS-all as ([A] + [L])/([V] + [A] + [Lx] + [L]). $P < 0.0001$ for all fits. A single *light-10* sample containing a small amount of Z was not included in the analysis.

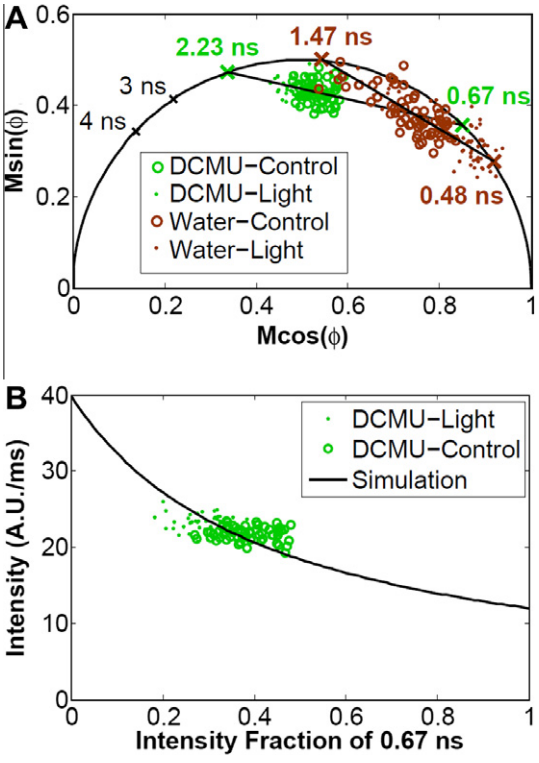

Fig. 9. (A) Polar plot analysis of FLIM data from leaf discs treated with water or 1.2 mM DCMU. Sample discs were floated on the DCMU solution for 360 min following a 20-min exposure to ~5 (*DCMU-control*, green open circles) or 400–500 µmol photons m^{-2} s^{-1} (*DCMU-light*, green filled circles). Data from leaf discs with the same treatment, but floating on water instead of DCMU, are also plotted (*water-control* and *water-light*, brown symbols). (B) Simulated fluorescence intensity corresponding to the polar plot analysis of DCMU-treated samples in (A) assuming two lifetime pools – see text for details. (For interpretation of the references to colour in this figure legend, the reader is referred to the web version of this article.)

stark contrast to the fluorescence quenching observed during the early part of the P–S–M phase of the Chl *a* fluorescence transient in all samples without DCMU (Fig. 4), which was interpreted as interconversion between the 1.5-ns and 0.5-ns lifetime pools based on the polar plot analysis (Fig. 6, see also data of water-treated samples in Fig. 9A). The polar plot points from all five samples in Fig. 9A (as mentioned above, the polar plot locations for each sample remained constant, but there were small differences between each sample) were fitted by linear regression giving a straight line that intercepted the semicircle at 2.23 and 0.67 ns (Fig. 9A), rather than 1.5 and 0.5 ns (Fig. 6 and water-treated samples in Fig. 9A). This result signifies a substantial increase in the fluorescence lifetime of the long lifetime pool from 1.5 to 2.2 ns. The small difference in the fast lifetime intercept (0.7 rather than 0.5 ns) is probably not significant due to error in the long straight-line extrapolation for data of the DCMU experiment. However, as shown by the location of the polar plot points, the short lifetime pool (0.7 ns) was already present in both *DCMU-control*- and *DCMU-light*-samples at the 1st FLIM measurements. This behavior of the species fraction of the rapid 0.7-ns lifetime pool in the DCMU-treated samples contrasts with the highly variable light-induced species fraction found for the short 0.5-ns lifetime pool in the samples without DCMU (Figs. 5 and 6).

Unlike uncouplers, which abolish ΔpH [18,42], DCMU inhibits linear electron transport and associated ΔpH, but does not block ΔpH build-up arising through cyclic electron transport around PSI [43,44]. Yet, lack of extensive light-induced fluorescence quenching in the DCMU-treated samples (Fig. 9) indicates that ΔpH-dependent quenching induced by cyclic electron transport (which DCMU cannot block) was negligible in the avocado leaves in our experiments. The low light could be the reason for the negligible cyclic electron flow. In fact, low cyclic electron transport activities have been measured in leaves of low-light grown plants and/or under low light intensities [45,46]. Limitation of PSI cyclic electron transport, together with inhibition of linear electron transport and resulting ΔpH formation, could explain the lack of

Please cite this article in press as: S. Matsubara et al., Photosystem II fluorescence lifetime imaging in avocado leaves: Contributions of the lutein-epoxide and violaxanthin cycles to fluorescence quenching, J. Photochem. Photobiol. B: Biol. (2011), doi:10.1016/j.jphotobiol.2011.01.003

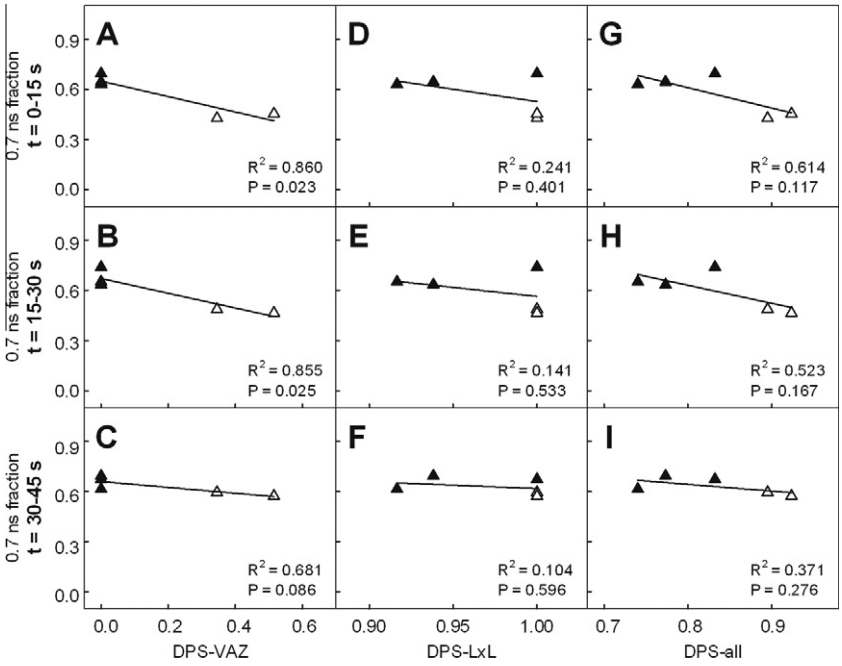

Fig. 10. Correlation between the de-epoxidation state (DPS) of the two xanthophyll cycles and the species fraction of the 0.7-ns lifetime pool in the *DCMU-control*- (filled symbols) and *DCMU-light*-samples (empty symbols) after a 360-min DCMU treatment. (A–C) De-epoxidation state of the V cycle, DPS-VAZ; (D–F) de-epoxidation state of the Lx cycle, DPS-LxL; (G–I) combined de-epoxidation state of the two cycles, DPS-all. The species fractions at the 1st (between 0 and 15 s; A, D and G), 2nd (between 15 and 30 s; B, E and H) and 3rd (between 30 and 45 s; C, F and I) measurements of the 21 FLIM measurements are shown. Each symbol represents an individual leaf disc. Zeaxanthin was detected in none of these samples.

light-induced fluorescence quenching in the DCMU-treated leaves of low-light acclimated avocado plants observed by using low-intensity blue excitation laser. While we cannot rule out the possibility that cyclic electron transport was activated transiently in dark-adapted, DCMU-treated avocado leaves in the first few seconds of illumination, as has been previously reported in leaves of spinach [43] and barley [44], such transient effects would hardly affect our results taken during the 5-min continuous FLIM measurements.

Similar responses found in *DCMU-control*- and *DCMU-light*-samples suggest that DPS may not influence fluorescence lifetimes of Chl *a* in the presence of DCMU. Indeed, in marked contrast to Fig. 8, in which the species fraction of the 0.5-ns lifetime pool was strongly correlated with DPS of the two xanthophyll cycles, there was no obvious, consistent correlation in the DCMU-treated samples between the species fraction of the 0.7-ns lifetime pool and any of the three DPS parameters (Fig. 10). The correlation between DPS-VAZ and the 0.7-ns pool was even slightly negative, if any. The DPS values varied greatly among the DCMU-treated samples, with DPS-VAZ ranging between 0 and 0.5 and DPS-LxL between 0.9 and 1.0. Yet, regardless of the extent of de-epoxidation in the two xanthophyll cycles, the 0.7-ns lifetime pool accounted for about 50–60% of the whole population of the fluorescing molecules in the DCMU-treated samples, implying that neither DPS-VAZ nor DPS-LxL was involved in this quenching.

4. Discussion

We have measured the lifetime-resolved fluorescence emission from intact, fully functional avocado leaves during the fluorescence transient at different times following initial light exposure. Analysis of the lifetime-resolved data is consistent with an interconversion between two lifetime pools (1.5 ns and 0.5 ns), representing different extents of Chl *a* quenching. This quenching dynamics is interpreted as a protective response of the plant to light exposure, linked with the V and Lx cycles. By carrying out lifetime-resolved measurements we could quantify changes in concentrations of the two quenched species of Chl *a* during the fluorescence transient. The relative molecular fractions determined from these fluorescence measurements have been correlated with DPS of the two cycles determined by HPLC measurements.

4.1. Slow phase of the Chl a fluorescence transient in avocado leaves

Our FLIM measurements tracked changes in Chl *a* fluorescence lifetimes during the P–S–M phase of the fluorescence transient in avocado leaves (Fig. 4). The decreasing fluorescence intensity in the first minutes clearly shows the P-to-S phase. This part of the fluorescence transient reflects the build-up of ΔpH [47], consistent with its absence following treatment with DCMU (Fig. 9A). In higher plants, the S-to-M rise, which follows the P-to-S decline, is observed under relatively low light intensities applied after at least a few minutes of darkness [48] and has been associated with photosynthetic induction [49]. In agreement with this, longer dark treatment delayed the onset of the S-to-M rise in both *control*- and *light*-samples (Fig. 4), suggesting a need of longer photosynthetic induction following prolonged darkness. This pronounced effect of darkness on the photosynthetic induction during the S-to-M phase contrasts with no apparent effect on the reactions in the P-to-S phase (see *control*-samples in Fig. 4).

Our FLIM measurements show that changes in the fluorescence intensity during the P–S–M transient can be well-accounted for by the interconversion of Chl *a* between longer (1.5 ns) and shorter (0.5 ns) fluorescence lifetime pools (Fig. 6B and C). This is in agreement with the earlier observation of parallel decline in the fluorescence yield and the average fluorescence lifetime in barley leaves during the qE-type quenching [37]. By using FLIM, we were able to identify and follow in real time the exchange of Chl molecules between two lifetime pools, in addition to detecting average lifetimes. Together with the disappearance of the P-to-S decrease in the intensity measurements (Fig. 9B) with the DCMU-treated samples, changes in the fluorescence lifetimes also vanished (Fig. 9A);

Please cite this article in press as: S. Matsubara et al., Photosystem II fluorescence lifetime imaging in avocado leaves: Contributions of the lutein-epoxide and violaxanthin cycles to fluorescence quenching, J. Photochem. Photobiol. B: Biol. (2011), doi:10.1016/j.jphotobiol.2011.01.003

the points on the polar plot clustered essentially randomly for the control and for the light samples. This suggests that these changes (without DCMU) in the lifetime pools are related to linear electron transport and resulting qE. Although fluorescence quenching by state transitions (qT) can take place on a time scale of the slow fluorescence transient, qT affects the fluorescence intensity by changing the *number* of Chl *a* molecules in PSII; fluorescence lifetimes do not depend on the concentrations of fluorophores, barring dimerization or aggregation. Since our simulation of the intensity solely from the polar plot analysis of lifetime data (assuming the number of fluorescing molecules remains constant and only the lifetimes change) fits the intensity data very well (Fig. 6C, and Appendix B, Fig. B.1), we conclude that the number of Chl *a* molecules attached to PSII did not change significantly during our FLIM measurements, and thus, we can disregard qT. A small PSII antenna size, as inferred from the relatively high ratios of Chl *a*/Chl *b* and carotene/xanthophyll (Table 1), may have restricted the extent of qT in our avocado leaves.

4.2. Fluorescence lifetime pools revealed by the polar plot

The polar plot analysis illustrates strikingly uniform light-induced transition patterns of the fluorescence lifetime parameters, M and φ, in both *control*- and *light*-samples (Fig. 6). A single straight-line fit of the data on the polar plot intersects the semicircle at locations corresponding to 0.5 and 1.5 ns. The FLIM measurements in avocado leaves in the wavelength region between 690 and 700 nm and between 715 and 725 nm yielded almost the same results as the measurements between 670 and 725 nm [28], confirming, as expected, that PSI makes only a very small contribution to the fluorescence at room temperature [29].

Our polar plot analysis of the FLIM data indicates a progressive change with illumination along a straight line between the two lifetime pools (1.5 and 0.5 ns, Fig. 6). For complex 3-D samples such as leaves, having spatial heterogeneity of fluorescence intensity (Fig. 2A) [25,41], we note that the data are mean values of heterogeneous areas (cf. Fig. 2B). Variations between the samples can lead to an average lifetime for each lifetime *pool*, which may consist of a distribution of similar lifetime components constituting a pool. We note that such pools of distributed lifetimes behave on the polar plot in the same way as expected for pools with singular lifetimes [31]; the intercept on the semicircle represents the average lifetime of the distribution.

4.3. Comparisons with other plant and algal systems

It is informative to compare our FLIM studies with avocado with earlier lifetime studies on algae and different plants. The PSII fluorescence lifetimes obtained in this study for avocado leaves are similar to the values reported for other higher-plant species.

Fluorescence lifetimes have been measured in leaves of cherry laurel during the Chl *a* fluorescence transient by using a phase and modulation fluorometer [50,51]. By assuming a three-exponential model, including a PSI component with a fixed lifetime of 0.08 ns, Moise and Moya [51] found two PSII lifetime components. The lifetimes of both PSII components decreased from P to S, namely from 2.4 to 1.19 ns for the longer one and from 0.96 to 0.4 ns for the shorter one.

By using a phase and modulation fluorometer and assuming a Lorentzian lifetime distribution model, Gilmore et al. [42,52,53] found two lifetime components, a longer one 1.6–2.1 ns and a shorter one 0.3–0.5 ns, in isolated thylakoids of spinach, lettuce and barley at the maximal fluorescence intensity in the presence of ΔpH (Fm′). In the absence of ΔpH (Fm), the same thylakoid samples showed a single major lifetime component at 2.0–2.4 ns. The two lifetime components at Fm′ and the main component at Fm obtained in these studies are comparable with the 1.5- and 0.5-ns pools that appeared in the polar plot of our *control*- and *light*-samples (Fig. 6A) and the 2.2-ns pool found in our DCMU experiment (Fig. 9A), respectively.

Wagner et al. [54] and Richter et al. [55] have identified three PSII fluorescence decay components in isolated pea thylakoids, in addition to two very fast decay components arising from PSI. They used a single photon counting method, combined with a global lifetime analysis and a target analysis. In "*closed*" PSII in a dark-adapted state (Fm), the PSII fluorescence lifetime consisted of a slow (longer than 2.5 ns), a medium (between 1.5 and 1.8 ns) and a fast decay component (between 0.3 and 0.7 ns). All three components showed much faster decay in "*open*" PSII (Fo): 1.5, 0.6 and 0.3 ns for the slow, medium and fast component, respectively [54]. The slow component found in pea thylakoids at Fm is comparable with the 2.2-ns pool in our DCMU-treated samples (Fig. 9A). Likewise, in their case, the medium and fast decay components at Fm, or the slow and medium components at Fo, have lifetimes similar to our 1.5- and 0.5-ns pools of *control*- and *light*-samples (Fig. 6A). Without DCMU, our FLIM data, which were acquired under a light intensity of ~50 μmol photons m^{-2} s^{-1}, could include fluorescence signals from both open and closed PSIIs. Nonetheless, it is noteworthy that in our case the initial species fraction of the 0.5-ns lifetime pool was closely correlated with the DPS of the two xanthophyll cycles in avocado leaves (Fig. 8); such correlations with DPS are expected for quenching processes related to NPQ, but not for photochemical quenching and shifts in population of open and closed PSII centers.

Also, the lifetime of the 0.5-ns pool is very close to an NPQ-related 0.4-ns decay component revealed in leaves of *Arabidopsis* [56]. This decay component has a far-red enhanced spectrum, resembling the spectral feature of aggregated LHCII [57,58], and its formation requires PsbS and Z components [59].

Taken together, these previous studies, conducted on different plant species by using a variety of methods, all point to the presence of a major PSII fluorescence lifetime component between 1.5 and 2.5 ns at Fm, which diminishes upon illumination concomitant with the appearance or increase of two shorter lifetime components, with the shortest one being faster than 0.5 ns. Essentially the same picture emerged in our polar plot analysis of FLIM data measured in avocado leaves during the P–S–M phase of the Chl *a* fluorescence transient. Thus, we propose that these fluorescence lifetime features reflect the key components and processes of qE which are common to a wide variety of higher plants.

In contrast to this common behavior of higher plant species, a different picture has been observed in the green alga *Chlamydomonas reinhardtii* during the P–S–M phase [19]. Data of *Chlamydomonas* measured under low or high light intensities (300 or 2750 μmol photons m^{-2} s^{-1}) did not fall on a straight line in the polar plot. The distinctively different patterns found in the polar plots of avocado leaves (this study) and *Chlamydomonas* cells [19] most likely reflect different physiology of these two organisms, including mechanisms of non-photochemical quenching, NPQ. For example, *Chlamydomonas* displays pronounced qT [38,60] and accumulates qE-associated pigment-binding proteins LHCSRs [61], but does not express PsbS protein [62], which senses lumen acidification [63] and triggers qE rapidly in higher plants [64]. Clearly, the polar plot visualizes different patterns of fluorescence quenching and lifetime transitions in different photosynthetic cells and tissues.

4.4. Two xanthophyll cycles and quenching of PSII fluorescence lifetime

Earlier studies showed that ΔpH reduces the lifetime and/or fractional contribution of the longer (>2 ns) lifetime component of PSII [42,53,54]. In our study, this effect of ΔpH manifested itself

Please cite this article in press as: S. Matsubara et al., Photosystem II fluorescence lifetime imaging in avocado leaves: Contributions of the lutein-epoxide and violaxanthin cycles to fluorescence quenching, J. Photochem. Photobiol. B: Biol. (2011), doi:10.1016/j.jphotobiol.2011.01.003

in the fluorescence intensity mainly as the difference between the long lifetime pools found with DCMU (2.2 ns) and without DCMU (1.5 ns) and also as the virtual disappearance of light-induced transition of the long lifetime pool to the short lifetime pool (compare Figs. 5 and 6 with Fig. 9). The points on the polar plot in Fig. 9 cluster below the 1.5 ns location on the semicircle, indicating that the slow lifetime pool has significantly lengthened (estimated 2.2 ns from 1.5 ns); the extrapolation to the faster lifetime pool is approximately the same as in the absence of DCMU. These estimates have been attained by including the control and light sample data together in the linear regression. According to Gilmore et al. [42], accumulation of Z further decreases the fluorescence lifetime to give rise to a short lifetime component at 0.3–0.5 ns, analogous with the 0.5-ns lifetime pool in our *control*- and *light*-samples (Fig. 6A). Indeed, the species fraction of the 0.5-ns pool shortly after the dark-to-light transfer was correlated with DPS, especially the combined DPS of the two cycles (Fig. 8).

Unlike in the previous studies, however, the overall DPS of our dark-adapted avocado leaf discs was determined by A and "*photo-converted*" L (the majority of L was not involved in the Lx cycle), instead of Z. We note that it is difficult to define with certainty the fraction of the L pool engaged in the Lx cycle. The majority of L is regarded as constitutive, and hence not involved in the cycle, because the levels of L are usually higher than those of Lx. In all Lx-cycle species thus far examined, L is present at the highest level among all carotenoid pigments in photosynthetic tissues. The lowest ratio of L to Lx (L:Lx) has been found in deeply shaded mature leaves of tropical rainforest evergreen trees, *Inga sapindoides* (110:80) [65] and *Virola elongata* (90:60) [35]. These leaves had been in light intensities lower than 10–20 μmol photons m^{-2} s^{-1} for months. The situation is quite different for the V cycle, which can exist in a zero-DPS state (e.g. Fig. 3); in this case all A and Z molecules formed under illumination are considered to be "engaged in the cycle". Lutein, on the other hand, is always present in large amounts. The levels of L and Lx undergo short-term (minutes to hours) and long-term (days to weeks and months) variations in leaves, depending on light environments [6,12]. The fraction of L (or Lx) involved in the cycle very likely changes during long-term acclimation. Moreover, pronounced differences in Lx content between young and mature leaves have been reported for avocado plants [15], suggesting additional effects during leaf development.

Because de-epoxidation of A to Z shortly after light exposure is supposedly minimal, the strong correlation found already in the first 15 s of illumination (Fig. 8A) suggests that A can significantly enhance the formation of the 0.5-ns lifetime pool [53]. The weaker correlation between DPS-LxL and the 0.5-ns pool (Fig. 8D–F) suggests a smaller effect due to photo-converted L compared to A. Nonetheless, the improved correlation of the 0.5-ns species fraction with DPS-all (Fig. 8G–I) indicates involvement of photo-converted L as well as A in the ΔpH-dependent interconversion between the 1.5- and 0.5-ns lifetime pools in avocado leaves. This is reminiscent of the rapid NPQ induction found in leaves of Lx-cycle plants after photo-conversion of Lx to L and in the absence of Z [12,13]. Acceleration of light-induced NPQ induction has also been reported in leaves of different mutants and transgenic plants of *Arabidopsis* with increased levels of Z or L. For instance, this has been reported for: *npq2* mutants accumulating Z due to the lack of Z epoxidase [5]; transgenic *lutOE* plants having an extra pool of L at the expense of V [8]; and *szl1npq1* double mutants in which a large part of the V pool is replaced by L and light-induced de-epoxidation in the V cycle is inhibited by mutation to V de-epoxidase [9].

We observed that the interconversion between the 1.5- and 0.5-ns pools was partly reversible during the S-to-M phase in both *control*- and *light*-samples (Figs. 5 and 6), which have different levels of DPS (Fig. 3). For efficient photosynthesis and flexible regulation of energy dissipation under low or fluctuating light conditions, it is necessary that fluorescence quenching be reversible: (1) concomitant with decreasing ΔpH, and (2) without a simultaneous decrease in DPS. The sensitivity to ΔpH for (1) is presumably ensured by PsbS [63,64], while the DPS-independent qE decline for (2) requires that de-epoxidized xanthophylls do not stabilize the quenched state (that is, the 0.5-ns lifetime pool). The partial reversion of fluorescence quenching during the light induction (Figs. 4–6) and the disappearance of DPS effects in the DCMU-treated samples (Figs. 8 and 9) suggest that retention of A and photo-converted L *per se* does not stabilize quenching. This behavior is similar to previous reports in sun and shade leaves of Lx-cycle species, showing comparably high maximal PSII efficiency despite large variations in DPS-LxL [12,13]. The minor intensity contribution of the 0.7-ns lifetime pool persisting in the DCMU-treated samples (Fig. 9B) independently of the variations in DPS (Fig. 10) may be attributed to quenching by oxidized plastoquinones [37] and/or photoinactivated PSII [55,66,67].

Stabilizing quenching by Z has been proposed from observations that the slow phase of NPQ relaxation (relaxing within 5–15 min in the dark, often treated as part of qI) is correlated with Z epoxidation (or retention) in leaves of different *Arabidopsis* mutants [5,7]. Likewise, the Z-dependent chronic quenching of PSII is a symptom observed in *npq2* mutants of *Arabidopsis* [18,20,21] as well as *Chlamydomonas* [19]. Although quenching stabilization can be beneficial under constant and/or prolonged stress, such as in overwintering evergreen leaves [16,17], it would cause wasteful energy dissipation when photosynthesis operates under mostly low but dynamic light environments characterized by occasional increase in irradiance [20].

5. Conclusions

Our real-time, continuously observed FLIM measurements on intact avocado leaves during light induction, in conjunction with our polar plot analysis, revealed the following: (1) the presence of two PSII fluorescence lifetime pools (1.5 ns and 0.5 ns in the absence of inhibitors, and 2.2 ns and 0.7 ns in the presence of DCMU); (2) the fluorescence intensity decrease, during fluorescence transient, from the P to S level correlates well with the conversion of the 1.5-ns pool to the 0.5-ns pool, and the opposite during the S to M fluorescence rise; (3) a correlation exists between retention of photo-converted L in the Lx cycle and A in the V cycle with the species fraction of the 0.5-ns lifetime pool upon illumination; and (4) there is requirement of ΔpH for the quenching effects of L and A. Based on our results we clearly demonstrate in this paper that both lutein and zeaxanthin cycles are involved in photoprotection in avocado leaves. However, because ΔpH cannot be controlled easily *in vivo*, and we do not know the precise pH dependence of each cycle *in vivo*, it is difficult to separate the contributions of the two cycles. While the difference between the correlations of DPS-LxL, DPS-VAZ and DPS-all (especially between the latter two) in Fig. 8 are small, the striking change from Fig. 8 (without DCMU) to Fig. 10 (with DCMU) indicates that L (and A) may not cause qI. Therefore, we propose that L and A do not quantitatively affect the fluorescence lifetimes in the presence of DCMU. Finally, the improved correlation of the 0.5-ns species fraction with DPS-all (see Fig. 8) indicates involvement of photo-converted L as well as A in the ΔpH-dependent interconversion between the 1.5- and 0.5-ns lifetime pools in avocado leaves.

Acknowledgements

The research stay of S.M. at University of Illinois at Urbana-Champaign was supported by a Deutsche Akademische

Austauschdienst (DAAD) travel grant (PPP-USA, D/07/10566). Y.-C.C. was supported by the Taiwan Merit Scholarships (TMS-094-1-A-036). G. was supported by the Department of Plant Biology at the University of Illinois at Urbana-Champaign. We thank Kelly Gillespie and Lisa Ainsworth (Department of Plant Biology, University of Illinois at Urbana-Champaign) for their help in freeze-drying the leaf disc samples. R.M.C. thanks the Research Board at UIUC for support. Although data were not included in this work, friendly and expert assistance by Mayandi Sivaguru (Microscopy and Imaging Facility, Institute for Genomic Biology, University of Illinois at Urbana-Champaign) for spinning disc confocal microscopy experiments is greatly acknowledged.

Appendix A

A.1. The two-lifetime model

In the two-lifetime model the fractions of molecular species undergoing interconversion between two states with different lifetimes are calculated from the lifetime parameters. The measured fluorescence response $F_\delta(t)$ of a two-lifetime system to a very short excitation pulse (a so called δ-function excitation pulse) is:

$$F_\delta(t) = a_1 \cdot \exp\left(-\frac{t}{\tau_1}\right) + a_2 \cdot \exp\left(-\frac{t}{\tau_2}\right) = (a_1 + a_2) \cdot \left[A_1 \cdot \exp\left(-\frac{t}{\tau_1}\right) + A_2 \cdot \exp\left(-\frac{t}{\tau_2}\right)\right]. \quad (A.1)$$

τ_1 and τ_2 are the two lifetimes. a_1 and a_2 are the corresponding pre-exponential factors, which are proportional to both the number of fluorescent molecules of each fluorescent component in the sample and the corresponding intrinsic radiative kinetic rate constant of each fluorescent component. In our calculation, the two lifetime components are derived from the same molecular species, but they have different lifetimes because they are in different environments (states or lifetime pools). Therefore, the intrinsic natural radiative rate constants are the same, and the pre-exponential factors are proportional to the number of molecules in each state. A_1 and A_2 are the fractional pre-exponential factors ($A_1 = \frac{a_1}{a_1+a_2}$ and $A_2 = \frac{a_2}{a_1+a_2}$), which are equal to the fractional concentrations of the fluorescent molecules in each environment (state).

In the frequency domain FLIM measurement, the excitation light $E(t)$ is repetitively modulated at a frequency ω and phase φ^E. $E(t)$ can be represented (in complex exponential notation) by:

$$Et = E_0 + E_\omega e^{j(\omega t + \varphi^E)}. \quad (A.2)$$

Here we have assumed that the excitation light is modulated by a single repetitive sinusoidal wave form (if the excitation is not a pure sinusoidal form, this procedure can be extended to be any Fourier component of the repetitive wave form). The emitted fluorescence signal following excitation by sinusoidally modulated excitation light is the convolution in time of Eqs. (A.1) and (A.2). After carrying out the convolution, the modulated fluorescence signal, $F_{\delta(t)} * E(t)$, becomes:

$$F_\delta(t) * E(t) = C \cdot (a_1 + a_2) \cdot \left[A_1\tau_1 \cdot \left(E_0 + \frac{E_\omega e^{j(\omega t+\varphi^E)}}{1+j\omega\tau_1}\right) + A_2\tau_2 \cdot \left(E_0 + \frac{E_\omega e^{j(\omega t+\varphi^E)}}{1+j\omega\tau_2}\right)\right] = C'' \cdot (A_1\tau_1 + A_2\tau_2) \cdot \left[f_1 \cdot (1 + M_1\cos(\varphi_1 + \varphi^E)) + f_2 \cdot (1 + M_2\cos(\varphi_2 + \varphi^E))\right], \quad (A.3)$$

where C accounts for the instrument factors of the FLIM instrument, and C'' is equal to $C \cdot E_0 \cdot (a_1 + a_2)$. In Eq. (A.3), the modulations (M_1, M_2) and phase (φ_1, φ_2) values are the same as defined earlier in the paper. f_1 and f_2 represent the fractional fluorescence intensities contributed by lifetime components τ_1 and τ_2, respectively. They are related to the fractional pre-exponential factors by the following equations:

$$f_1 = \frac{A_1\tau_1}{A_1\tau_1 + A_2\tau_2}, \quad (A.4)$$

$$f_2 = \frac{A_2\tau_2}{A_1\tau_1 + A_2\tau_2}. \quad (A.5)$$

For the two-lifetime model, least-square fitting of the polar plot data to a straight line is carried out to determine the fractional intensities f_1 and f_2 and the two lifetimes τ_1 and τ_1 (the lifetimes are related to the intercepts of the straight line with the semicircle). The fractional pre-exponential factors A_1 and A_2 are derived from f_1 and f_2 using Eqs. (A.4) and (A.5). Using these values, the steady state fluorescence intensity, $C'' \cdot (A_1\tau_1 + A_2\tau_2)$, can be simulated and compared to the measured fluorescence intensities. This is a good test for the applicability of the two component model. C'' is just a constant that is varied to give the best fit to the measured fluorescence intensity.

Appendix B. Supplementary material

Supplementary data associated with this article can be found, in the online version, at doi:10.1016/j.jphotobiol.2011.01.003.

References

[1] Govindjee, J.F. Kern, J. Messinger, J. Whitmarsh, Photosystem II, in: Encyclopedia of Life Sciences, John Wiley & Sons, Chichester, 2010, <www.els.net>.
[2] B. Demmig-Adams, W.W. Adams III, The role of xanthophyll cycle carotenoids in the protection of photosynthesis, Trends Plant. Sci. 1 (1996) 21–26.
[3] P. Müller, X.-P. Li, K.K. Niyogi, Non-photochemical quenching, a response to excess light energy, Plant Physiol. 125 (2001) 1558–1566.
[4] W. Bilger, O. Björkman, S.S. Thayer, Light-induced spectral absorbance changes in relation to photosynthesis and the epoxidation state of xanthophyll cycle components in cotton leaves, Plant Physiol. 91 (1989) 542–551.
[5] K.K. Niyogi, A.R. Grossman, O. Björkman, *Arabidopsis* mutants define a central role for the xanthophyll cycle in regulation of photosynthetic energy conversion, Plant Cell 10 (1998) 1121–1134.
[6] J.I. García-Plazaola, S. Matsubara, C.B. Osmond, The lutein epoxide cycle in higher plants: its relationships to other xanthophyll cycles and possible functions, Funct. Plant Biol. 34 (2007) 759–773.
[7] B.J. Pogson, K.K. Niyogi, O. Björkman, D. DellaPenna, Altered xanthophyll compositions adversely affect chlorophyll accumulation and nonphotochemical quenching in *Arabidopsis* mutants, Proc. Natl. Acad. Sci. USA 95 (1998) 13324–13329.
[8] B.J. Pogson, H.M. Rissler, Genetic manipulation of carotenoids biosynthesis and photoprotection, Philos. Trans. Roy. Soc. Lond. B 355 (2000) 1395–1403.
[9] Z. Li, T.K. Ahn, T.J. Avenson, M. Ballottari, J.A. Cruz, D.M. Kramer, R. Bassi, G.R. Fleming, J.D. Keasling, K.K. Niyogi, Lutein accumulation in the absence of zeaxanthin restores nonphotochemical quenching in the *Arabidopsis thaliana npq1* mutant, Plant Cell 21 (2009) 1798–1812.
[10] A.V. Ruban, R. Berera, C. Ilioaia, I.H.M. van Stokkum, J.T.M. Kennis, A.A. Pascal, H. van Amerongen, B. Robert, P. Horton, R. van Grondelle, Identification of a mechanism of photoprotective energy dissipation in higher plants, Nature 450 (2007) 575–578.
[11] A.A. Pascal, Z. Liu, K. Broess, B. van Oort, H. van Amerongen, C. Wang, P. Horton, B. Robert, W. Chang, A. Ruban, Molecular basis of photoprotection and control of photosynthetic light-harvesting, Nature 436 (2005) 134–137.
[12] S. Matsubara, G.H. Krause, M. Seltmann, A. Virgo, T.M. Kursar, P. Jahns, K. Winter, Lutein epoxide cycle, light harvesting and photoprotection in species of the tropical tree genus *Inga*, Plant Cell Environ. 31 (2008) 548–561.
[13] R. Esteban, S. Matsubara, M.S. Jiménez, D.D. Morales, P. Brito, R. Lorenzo, B. Fernández-Marín, J.M. Becerril, J.I. García-Plazaola, Operation and regulation of lutein epoxide cycle in seedlings of *Ocotea foetens*, Funct. Plant Biol. 37 (2010) 859–869.
[14] J.I. García-Plazaola, A. Hernández, J.M. Olano, J.M. Becerril, The operation of the lutein epoxide cycle correlates with energy dissipation, Funct. Plant Biol. 30 (2003) 319–324.
[15] B. Förster, C.B. Osmond, B.J. Pogson, De novo synthesis and degradation of Lx and V cycle pigments during shade and sun acclimation in avocado leaves, Plant Physiol. 149 (2009) 1179–1195.

[16] W.W. Adams III, B. Demmig-Adams, A.S. Verhoeven, D.H. Barker, 'Photoinhibition' during winter stress: involvement of sustained xanthophyll cycle-dependent energy dissipation, Aust. J. Plant Physiol. 22 (1994) 261–276.
[17] A.M. Gilmore, M.C. Ball, Protection and storage of chlorophyll in overwintering evergreens, Proc. Natl. Acad. Sci. USA 97 (2000) 11098–11101.
[18] L. Dall'Osto, S. Caffarri, R. Bassi, A mechamism of nonphotochemical energy dissipation, independent from PsbS, revealed by a conformational change in the antenna protein CP26, Plant Cell 17 (2005) 1217–1232.
[19] O. Holub, M.J. Seufferheld, C. Gohlke, Govindjee, G.J. Heiss, R.M. Clegg, Fluorescence lifetime imaging microscopy of *Chlamydomonas reinhardtii*: non-photochemical quenching mutants and the effect of photosynthetic inhibitors on the slow chlorophyll fluorescence transients, J. Microsc. 226 (2007) 90–120.
[20] L. Kalituho, J. Rech, P. Jahns, The roles of specific xanthophylls in light utilization, Planta 225 (2007) 423–439.
[21] M.P. Johnson, M.L. Pérez-Bueno, A. Zia, P. Horton, A.V. Ruban, The zeaxanthin-independent and zeaxanthin-dependent qE components of nonphotochemical quenching involve common conformational changes within the photosystem II antenna in Arabidopsis, Plant Physiol. 149 (2009) 1061–1075.
[22] Govindjee, Sixty-three years since Kautsky: chlorophyll *a* fluorescence, J. Plant Physiol. 22 (1995) 131–160.
[23] G.C. Papageorgiou, M. Tsimilli-Michael, K. Stamatakis, The fast and slow kinetics of chlorophyll a fluorescence induction in plants, algae and cyanobacteria: a viewpoint, Photosynth. Res. 94 (2007) 275–290.
[24] U. Noomnarm, R.M. Clegg, Fluorescence lifetimes: fundamentals and interpretations, Photosynth. Res. 101 (2009) 181–194.
[25] O. Holub, M.J. Seufferheld, C. Gohlke, Govindjee, R.M. Clegg, Fluorescence lifetime imaging (FLI) in real-time – a new technique in photosynthesis research, Photosynthetica 38 (2000) 581–599.
[26] S.L. Harmer, J.B. Hogenesch, M. Straume, H.-S. Chang, B. Han, T. Zhu, X. Wang, J.A. Kreps, S.A. Kay, Orchestrated transcription of key pathways in Arabidopsis by the circadian clock, Science 290 (2000) 2110–2113.
[27] B.R. Velthuys, Electron-dependent competition between plastoquinones and inhibitors for binding to photosystem II, FEBS Lett. 126 (1981) 277–281.
[28] Y.-C. Chen, R.M. Clegg, Fluorescence lifetime-resolved imaging, Photosynth. Res. 102 (2009) 143–155.
[29] E. Pfündel, Estimating the contribution of photosystem I to total leaf fluorescence, Photosynth. Res. 56 (1998) 185–195.
[30] P.C. Schneider, R.M. Clegg, Rapid acquisition, analysis, and display of fluorescence lifetime-resolved images for real-time applications, Rev. Sci. Instrum. 68 (1997) 4107–4119.
[31] G.I. Redford, R.M. Clegg, Polar plot representation for frequency-domain analysis of fluorescence lifetimes, J. Fluoresc. 15 (2005) 805–815.
[32] A.H.A. Clayton, Q.S. Hanley, P.J. Verveer, Graphical representation and multicomponent analysis of single-frequency fluorescence lifetime imaging microscopy data, J. Microsc. 213 (2004) 1–5.
[33] A.M. Gilmore, H.Y. Yamamoto, Resolution of lutein and zeaxanthin using a non-endcapped, lightly carbon-loaded C18 high-performance liquid chromatographic column, J. Chromatogr. 543 (1991) 137–145.
[34] A. Färber, P. Jahns, The xanthophyll cycle of higher plants: influence of antenna size and membrane organization, Biochim. Biophys. Acta 1363 (1998) 47–58.
[35] S. Matsubara, G.H. Krause, J. Aranda, A. Virgo, K.G. Beisel, P. Jahns, K. Winter, Sun-shade patterns of leaf carotenoid composition in 86 species of neotropical forest plants, Funct. Plant Biol. 36 (2009) 20–36.
[36] S. Matsubara, T. Morosinotto, C.B. Osmond, R. Bassi, Short- and long-term operation of the lutein-epoxide cycle in light-harvesting antenna complexes, Plant Physiol. 144 (2007) 926–941.
[37] B. Genty, Y. Goulas, B. Dimon, G. Peltier, J.M. Briantais, I. Moya, Modulation of efficiency of primary conversion in leaves, mechanisms involved at PS2, in: N. Murata (Ed.), Research in Photosynthesis, vol. 4, Kluwer Academic Publishers, Dordorecht, 1992, pp. 603–610.
[38] J.F. Allen, C.W. Mullineaux, Probing the mechanism of state transitions in oxygenic photosynthesis by chlorophyll fluorescence spectroscopy, kinetics and imaging, in: G.C. Papageorgiou, Govindjee (Eds.), Chlorophyll Fluorescence – A Signature of Photosynthesis, Springer, Dordorecht, 2004, pp. 447–461.
[39] M. Iwai, M. Yokono, N. Inada, J. Minagawa, Live-cell imaging of photosystem II antenna dissociation during state transitions, Proc. Natl. Acad. Sci. USA 107 (2009) 2337–2342.
[40] G.H. Krause, P. Jahns, Non-photochemical energy dissipation determined by chlorophyll fluorescence quenching: characterization and function, in: G.C. Papageorgiou, Govindjee (Eds.), Chlorophyll Fluorescence – A Signature of Photosynthesis, Springer, Dordorecht, 2004, pp. 463–495.
[41] N.R. Baker, Chlorophyll fluorescence: a probe of photosynthesis in vivo, Annu. Rev. Plant Biol. 59 (2008) 89–113.
[42] A.M. Gilmore, T.L. Hazlett, Govindjee, Xanthophyll cycle-dependent quenching of photosystem II chlorophyll a fluorescence: formation of a quenching complex with a short fluorescence lifetime, Proc. Natl. Acad. Sci. USA 92 (1995) 2273–2277.
[43] P. Joliot, A. Joliot, Cyclic electron transport in plant leaf, Proc. Natl. Acad. Sci. USA 99 (2002) 10209–10214.
[44] A.J. Golding, G. Finazzi, G.N. Johnson, Reduction of the thylakoid electron transport chain by stromal reductants – evidence for activation of cyclic electron transport upon dark adaptation or under drought, Planta 220 (2004) 356–363.
[45] A. Laisk, H. Eichelmann, V. Oja, R.B. Peterson, Control of cytochrome b_6f at low and high light intensity and cyclic electron transport in leaves, Biochim. Biophys. Acta 1708 (2005) 79–90.
[46] C. Miyake, S. Horiguchi, A. Makino, Y. Shinzaki, H. Yamamoto, K. Tomizawa, Effects of light intensity on cyclic electron flow around PSI and its relationship to non-photochemical quenching of Chl fluorescence in tobacco leaves, Plant Cell Physiol. 46 (2005) 1819–1830.
[47] J.-M. Briantais, C. Vernotte, M. Picaud, G.H. Krause, A quantitative study of the slow decline of chlorophyll a fluorescence in isolated chloroplasts, Biochim. Biophys. Acta 548 (1979) 128–138.
[48] M.N. Sivak, K.-J. Dietz, U. Heber, D.A. Walker, The relationship between light scattering and chlorophyll *a* fluorescence during oscillations in photosynthetic carbon assimilation, Arch. Biochem. Biophys. 237 (1985) 513–519.
[49] D.A. Walker, Secondary fluorescence kinetics of spinach leaves in relation to the onset of photosynthetic carbon assimilation, Planta 153 (1981) 273–278.
[50] N. Moise, I. Moya, Correlation between lifetime heterogeneity and kinetics heterogeneity during chlorophyll fluorescence induction in leaves: 1. Mono-frequency phase and modulation analysis reveals a conformational change of a PSII pigment complex during the lP thermal phase, Biochim. Biophys. Acta 1657 (2004) 33–46.
[51] N. Moise, I. Moya, Correlation between lifetime heterogeneity and kinetics heterogeneity during chlorophyll fluorescence induction in leaves: 2. Multi-frequency phase and modulation analysis evidences a loosely connected PSII pigment–protein complex, Biochim. Biophys. Acta 1657 (2004) 47–60.
[52] A.M. Gilmore, T.L. Hazlett, P.G. Debrunner, Govindjee, Photosystem II chlorophyll *a* fluorescence lifetimes and intensity are independent of the antenna size differences between barley wild-type and *chlorina* mutants: Photochemical quenching and xanthophyll cycle-dependent nonphotochemical quenching of fluorescence, Photosynth. Res. 48 (1996) 171–187.
[53] A.M. Gilmore, V.P. Shinkarev, T.L. Hazlett, Govindjee, Quantitative analysis of the effects of intrathylakoid pH and xanthophyll cycle pigments on chlorophyll *a* fluorescence lifetime distribution and intensity in thylakoids, Biochemistry 37 (1998) 13582–13593.
[54] B. Wagner, R. Goss, M. Richter, A. Wild, A.R. Holzwarth, Picosecond time-resolved study on the nature of high-energy-state quenching in isolated pea thylakoids. Different localization of zeaxanthin dependent and independent quenching mechanisms, J. Photochem. Photobiol. B 36 (1996) 339–350.
[55] M. Richter, R. Goss, B. Wagner, A.R. Holzwarth, Characterization of the fast and slow reversible components of non-photochemical quenching in isolated pea thylakoids by picoseconds time-resolved chlorophyll fluorescence analysis, Biochemistry 38 (1999) 12718–12726.
[56] Y. Miloslavina, A. Wehner, P.H. Lambrev, E. Wientjes, M. Reus, G. Garab, R. Croce, A.R. Holzwarth, Far-red fluorescence: a direct spectroscopic marker for LHCII oligomer formation in non-photochemical quenching, FEBS Lett. 582 (2008) 3625–3631.
[57] J.E. Mullet, C.J. Arntzen, Simulation of grana stacking in a model membrane system. Mediation by a purified light-harvesting pigment–protein complex from chloroplast, Biochim. Biophys. Acta 589 (1980) 100–117.
[58] P. Horton, M. Wentworth, A. Ruban, Control of the light harvesting function of chloroplast membranes: the LHCII-aggregation model for non-photochemical quenching, FEBS Lett. 579 (2005) 4201–4206.
[59] P.H. Lambrev, M. Nilkens, Y. Miloslavina, P. Jahns, A.R. Holzwarth, Kinetic and spectral resolution of multiple nonphotochemical quenching components in Arabidopsis leaves, Plant Physiol. 152 (2010) 1611–1624.
[60] R. Delosme, J. Olive, F.-A. Wollman, Changes in light energy distribution upon state transitions: an in vivo photoacoustic study of the wild type and photosynthesis mutants from *Chlamydomonas reinhardtii*, Biochim. Biophys. Acta 1273 (1996) 150–158.
[61] G. Peers, T.B. Truong, E. Ostendorf, A. Busch, D. Elrad, A.R. Grossman, M. Hippler, K.K. Niyogi, An ancient light-harvesting protein is critical for the regulation of algal photosynthesis, Nature 462 (2009) 518–521.
[62] G. Bonente, F. Passarini, S. Cazzaniga, C. Mancone, M.C. Buia, M. Tripodi, R. Bassi, S. Caffarri, The occurrence of the psbS gene product in *Chlamydomonas reinhardtii* and in other photosynthetic organisms and its correlation with energy quenching, Photochem. Photobiol. 84 (2008) 1359–1370.
[63] X.-P. Li, A.M. Gilmore, S. Caffarri, R. Bassi, T. Golan, D. Kramer, K.K. Niyogi, Regulation of photosynthetic light harvesting involves intrathylakoid lumen pH sensing by the PsbS protein, J. Biol. Chem. 279 (2004) 22866–22874.
[64] X.-P. Li, O. Björkman, C. Shih, A.R. Grossman, M. Rosenquist, S. Jansson, K.K. Niyogi, A pigment-binding protein essential for regulation of photosynthetic light harvesting, Nature 403 (2000) 391–395.
[65] S. Matsubara, M. Naumann, R. Martin, C. Nichol, U. Rascher, T. Morosinotto, R. Bassi, B. Osmond, Slowly reversible de-epoxidation of lutein-epoxide in deep shade leaves of a tropical tree legume may 'lock-in' lutein-based photoprotection during acclimation to strong light, J. Exp. Bot. 56 (2005) 461–468.
[66] I. Vass, G. Gatzen, A.R. Holzwarth, Picosecond time-resolved fluorescence studies on photoinhibition and double reduction of Q_A in photosystem II, Biochim. Biophys. Acta 1183 (1993) 388–396.
[67] S. Matsubara, W.S. Chow, Populations of photoinactivated photosystem II reaction centers characterized by chlorophyll *a* fluorescence lifetime in vivo, Proc. Natl. Acad. Sci. USA 101 (2004) 18234–18239.

Please cite this article in press as: S. Matsubara et al., Photosystem II fluorescence lifetime imaging in avocado leaves: Contributions of the lutein-epoxide and violaxanthin cycles to fluorescence quenching, J. Photochem. Photobiol. B: Biol. (2011), doi:10.1016/j.jphotobiol.2011.01.003